Characterization of molecular and metabolic phenotypes of *Clostridium* syntrophic co-culture

by

Yin Zou

A thesis submitted to the Faculty of the University of Delaware in partial fulfillment of the requirements for the degree of Degree in Major with Distinction

Spring 2022

Characterization of molecular and metabolic

phenotypes of *Clostridium* syntrophic co-culture

by

Yin Zou

Approved: 

Eleftherios Terry Papoutsakis, Ph.D.
Professor in charge of thesis on behalf of the Advisory Committee

Approved: 

Mark Alan Blenner, Ph.D.
Committee member from the Department of Chemical and Biomolecular Engineering

Approved: 

Monique Hite Head, Ph.D.
Committee member from the Board of Senior Thesis Readers

Approved: _____

Michael Chajes, Ph.D.
Chair of the University Committee on Student and Faculty Honors

ACKNOWLEDGMENTS

Firstly, I would like to thank Dr. Papoutsakis for providing me with this opportunity to conduct undergraduate research in his lab. Also, I would like to give my gratitude to my senior thesis committee members, Dr. Blenner and Dr. Head, for their support and feedback on my project and thesis. I would also like to thank my graduate student research mentors, Jonathan Otten, and Hannah Streett, for their patience during my training and tireless mentoring and guidance. I would also like to thank all the members of the Papoutsakis group, for their support and guidance.

Lastly, I would like to thank my family and friends for their support and accompany, without them I would never accomplish as much as I have accomplished today.

TABLE OF CONTENTS

LIST OF TABLES

LIST OF FIGURES

ABSTRACT

Historically, *Clostridium* species were used in Acetone-Butanol-Ethanol (ABE) fermentation. However, the ABE fermentation processes face competition from petroleum based processes, thus fermentation processes need to evolve to produce a higher valued chemical efficiently. *Clostridium* species are known to metabolize a range of sugar molecules and produce valuable chemicals such as hexanol and octanol. To achieve this goal, utilization of co-culture allows each species of bacteria to specialize in one task and avoids complex metabolism engineering. In this thesis, optimization of the bioreactor performance of syntrophic *Clostridium* co-culture for medium chain alcohol or fatty acid production utilizing *Clostridium kluvyeri* and *Clostridium saccharolyticum.* And the characterization of the molecular interactions and localization of proteins of interest related to cell-to-cell interaction was investigated. In the bioreactor investigation, the optimized *C. kluyveri* monoculture yielded 173 mM of hexanoate. In comparison the co-culture yielded 123 mM of hexanote. The result exhibits promising industrial value for *Clostridium* co-culture, and the insufficient supply of ethanol from C. *saccharolyticum* could be the major drawback for this co-culture system, which may be improved by incorporating a third species into the system such as *Clostridium ljungdahlii*.

Direct cell-to-cell material exchange between *Clostridium acetobutylicum* and *C. ljungdahlii* has been previously shown by our lab [1] This phenomenon greatly improves the productivity and carbon utilization in the co-culture, thus understanding the mechanism of cell-to-cell material exchange is critical to improve the performance of the co-culture and bring more industrial and economical significance. It is possible that *C. ljundahlii* could be actively seeking CO_2 rich source and therefore fused with

C. acetobutylicum to consume CO_2 waste produced by *C. acetobutylicum*. To further investigate this phenomenon, the localization pattern of the proteins of interest such as carbonic anhydrase (CA) and methyl-accepting chemotaxis protein (MCP) could be helpful. These proteins may be involved in CO_2 metabolism and CO_2 sensing respectively. To visualize the localization of these proteins, Halotag was fused with the two proteins of interest. The preliminary testing of the fluorescence of both MCP-Halotag and CA-Halotag under the microscope in *Escherichia coli* and under the flow cytometry in *C. ljungdahlii* shows the strong fluorescent intensity of the fluorescent fused protein. Visualizing the proteins in *C. ljungdahlii* under the microscopy, uniform membrane localization of MCP-Halotag and uniform cytoplasmic localization were observed. Future experiment of fluorescent imaging *C. acetobutylicum* and *C. ljungdahlii* utilizing the MCP-Halotag and CA-Halotag could provide more information about the proteins involved in the cell-to-cell direct material exchange.

Chapter 1

INTRODUCTION

1.1 Introduction to *Clostridium* species and their importance

Some *Clostridium* species are acetogens that fix CO_2 chemolithographically. Thus, *Clostridium* species possess many desirable traits for biotechnology application, as they are capable of utilize many organic substrates and produce a broad spectrum of useful metabolites. Therefore, studies on their characteristics and the techniques to engineer optimal behavior becomes crucial to utilize *Clostridium* species in bioprocessing.[2]

1.1.1 *Clostridium acetobutylicum* and Acetone-Butanol-Ethanol fermentation

C. acetobutylicum is a Gram-positive, spore-forming, obligately anaerobic organism that is a member of the solventogens. Solventogenic *Clostridium* species utilize a range of simple or complex sugars to produce solvents including acetone, butanol, and ethanol. In fact, one of the earliest fermentations utilized by man was acetone fermentation by solventogenic bacteria, and many solventogenic *Clostridium* species were isolated and used for Acetone-Butanol-Ethanol (ABE) fermentation.[3] ABE fermenting *Clostridium* species exhibit a biphasic growth pattern. In their early growth stages, acidogenic behavior can be observed, as the bacteria produces acetic acid and butyric acid. As the *Clostridium* culture reaches stationary growth phase, solventogenic behavior can be observed, the bacteria reabsorb and convert the acid into solvents.[2] Especially in *C. acetobutylicum* the stationary phase solventogenic

switch was observed with a morphological change in the cell and was reported at low pH the solvent production becomes prominent. [4] The solvent production switch of *C. acetobutylicum* was suggested to be caused by the pH reduction acid accumulated, as well as the ATP availability to the bacteria. [5] However, high concentration of solvent inhibits cell growth and leads to cell death. Thus, utilizing fed-batch fermentation to supply cells with supplemental nutrients and pH control as well as creating more butanol tolerant and higher solvent producing *C. acetobutylicum* strains would be desirable for ABE fermentation. However, ABE fermentation faces competition from petroleum-based processes. As the production cost of other routes is cheaper than *C. acetobutylicum* fermentation. The solventogenic nature of *C. acetobutylicum* make this strain of bacteria useful in applications such as *Clostridium* co-culture, which will be introduced later.

1.1.2 *Clostridium ljungdahlii* and the Wood Ljungdahl Pathway (WLP)

C. ljungdahlii are Gram-positive bacteria with a growth pH range of 4.0-7.0, but optimal growth at pH 6.0. *C. ljungdahlii* is an acetogen, meaning they can use an electron donor, such as H_2, to metabolize CO_2 as a sole carbon source.[6] *C. ljungdahlii* utilize the Wood Ljungdahl Pathway (WLP) for its primary metabolism which through carbonyl branch, that converts CO_2 into CO by CO dehydrogenase/Acetyl-CoA synthase complex (CODH/ACS) or via methyl branch CO_2 is reduced to formate, then to a methyl group. Both carbonyl and methyl branch are eventually converted to Acetyl- CoA by ACS, which the Acetyl-CoA produced from WLP would be used downstream to produce acid and solvents and ATP generation. *C. ljungdahlii* can also use the hexose fructose (but not glucose) via glycolysis to generate ATP for growth

through substrate-level phosphorylation.[2] Due to the CO_2 fixing nature the *C. ljungdahlii* could be an ideal partner for solventogens in syntrophic co-cultures. [7]

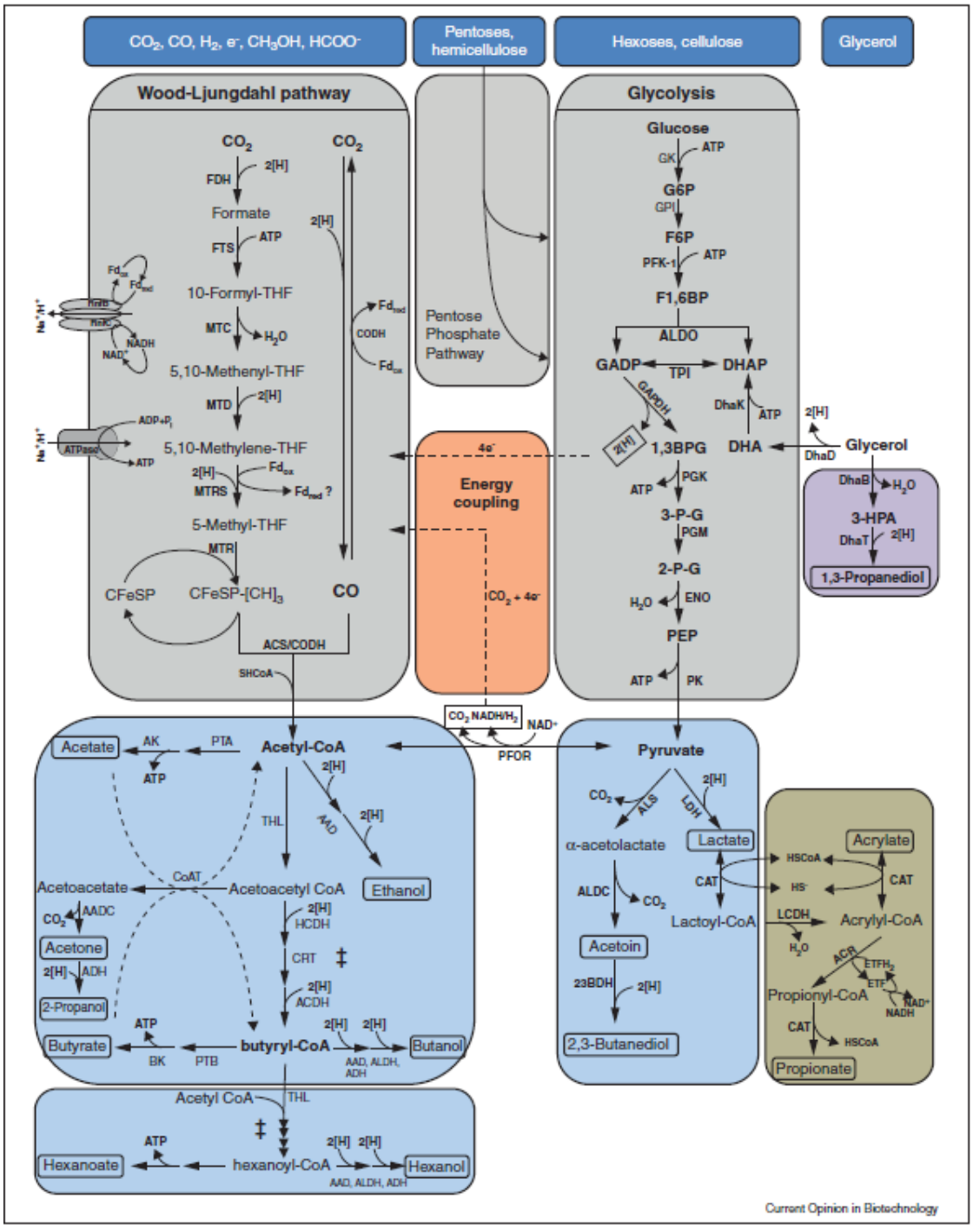

Figure.1.1 Scheme of metabolic pathways, energy conservation and metabolite production in *Clostridia*. Glycolysis, the pentose phosphate pathway, and the Wood–Ljungdahl pathway necessary for growth on hexoses, pentoses and syngas respectively, are shown in gray. Substrates used by these pathways are shown in dark blue boxes at the top and products are circled in black. Pathways involved in conversion of acetyl-CoA and pyruvate are shown in light blue. Production of 1,3-propanediol from glycerol is shown in purple, and production pathways for propionate and acrylate are shown in brown. Energy coupling between glycolysis and WL-pathway is in orange. The z indicates that the same enzyme reactions are involved in production of both butyryl-CoA and hexanoyl-CoA. Abbreviations of the different metabolites or enzymes are as follows: 23BDH, 2,3-butanediol dehydrogenase; AAD, alcohol/aldehyde dehydrogenase; AADC, acetoacetate decarboxylase; ACDH, acyl-CoA dehydrogenase; ACR, acrylyl-CoA reductase; ACS/CODH, acetyl-CoA synthase/CO dehydrogenase; ADH, alcohol dehydrogenase; AK, acetate kinase; ALDC, acetolactate decarboxylase; ALDH,aldehyde dehydrogenase; ALDO, fructose biphosphate aldolase; ALS, acetolactate synthase; BK, butyrate kinase; CAT, CoA transferase; CFeSP,corrinoid iron–sulfur protein; CRT, crotonase; DhaB, glycerol dehydratase; DhaD, glycerol dehydratase; DhaK, DHA kinase; DhaT, 1,3-propanedioloxidoreductase; ENO, enolase; Etf, electron-transferring flavoprotein; Fd, ferredoxin; FDH, formate dehydrogenase; FTS, formyl-THF synthase;GAPDH, glyceraldehyde phosphate dehydrogenase; GK, hexokinase; GPI, phosphoglucose isomerase; HCDH, 3-hydroxyacyl-CoAdehydrogenase;LCDH, lactoyl-CoA dehydrogenase; LDH, lactate dehydrogenase; MTC, methenyl-THF cyclohydrolase; MTD, methylene-THF dehydrogenase; MTR, methyl transferase; MTRS, methylene-THF reductase; PFK-1, phosphofructokinase; PFOR, pyruvate: ferredoxin oxidoreductase; PGK, phosphoglycerate kinase; PGM, phosphoglycerate mutase; PK, pyruvate kinase; PTA, phosphotransacetylase; PTB, phosphotransbutyrylase; THL, thiolase; TPI, triosephosphate isomerase. Figure reproduced from Tracy et al (2012)

1.1.3 *Clostridium kluyveri* and fatty acid chain elongation

C. kluyveri is a obligate anaerobic and is Gram variable but mostly Gram-negative *Clostridium* bacterium.[8] *C. kluyveri* has a growth pH range of 6.0 to 7.5, and have mild growth inhibition at more acidic pH 5.5. [9] *C. kluyveri* does not grow on

sugars. Instead, in the presence of CO_2 or bicarbonate *C. kluyveri* grows on short chain alcohols and carboxylic acids. Notably it grows ethanol and acetate forming butyrate, caproate (hexanoate) and H_2 gas. It can also extend the reaction further to form octanoate, and when fed ethanol and propionate to form pentanoate and heptanoate. [7]

The fermentation of ethanol + acetate starts with the oxidation of ethanol via a NAD-dependent ethanol dehydrogenase (Adh) and an NAD(P)-dependent acetaldehyde dehydrogenase (Ald) to forms acetyl-CoA. Using a chain of enzymes, including acetoacetyl-CoA thiolase (Thl), NAD- and NADP-dependent 3-hydroxybutyryl-CoA dehydrogenase (Hbd), 3-hydroxybutyryl-CoA dehydrogenase (Hbd), 3-hydroxybutyryl-CoA dehydratase (Crt) and NAD-dependent butyryl-CoA dehydrogenase complex (Bcd/EtfAB) and butyryl-CoA: acetate CoA transferase (Cat3) acetyl-CoA can form butyryl-CoA, and further acetate can replace the butyryl-CoA to yield butyrate and fresh acetyl-CoA.[8] To elongate the fatty acid chain reverse beta oxidation is utilized, so that 2 carbons from acetyl-CoA can be added, forming products from four carbon butyrate to eight carbon caprylic acid. [9]

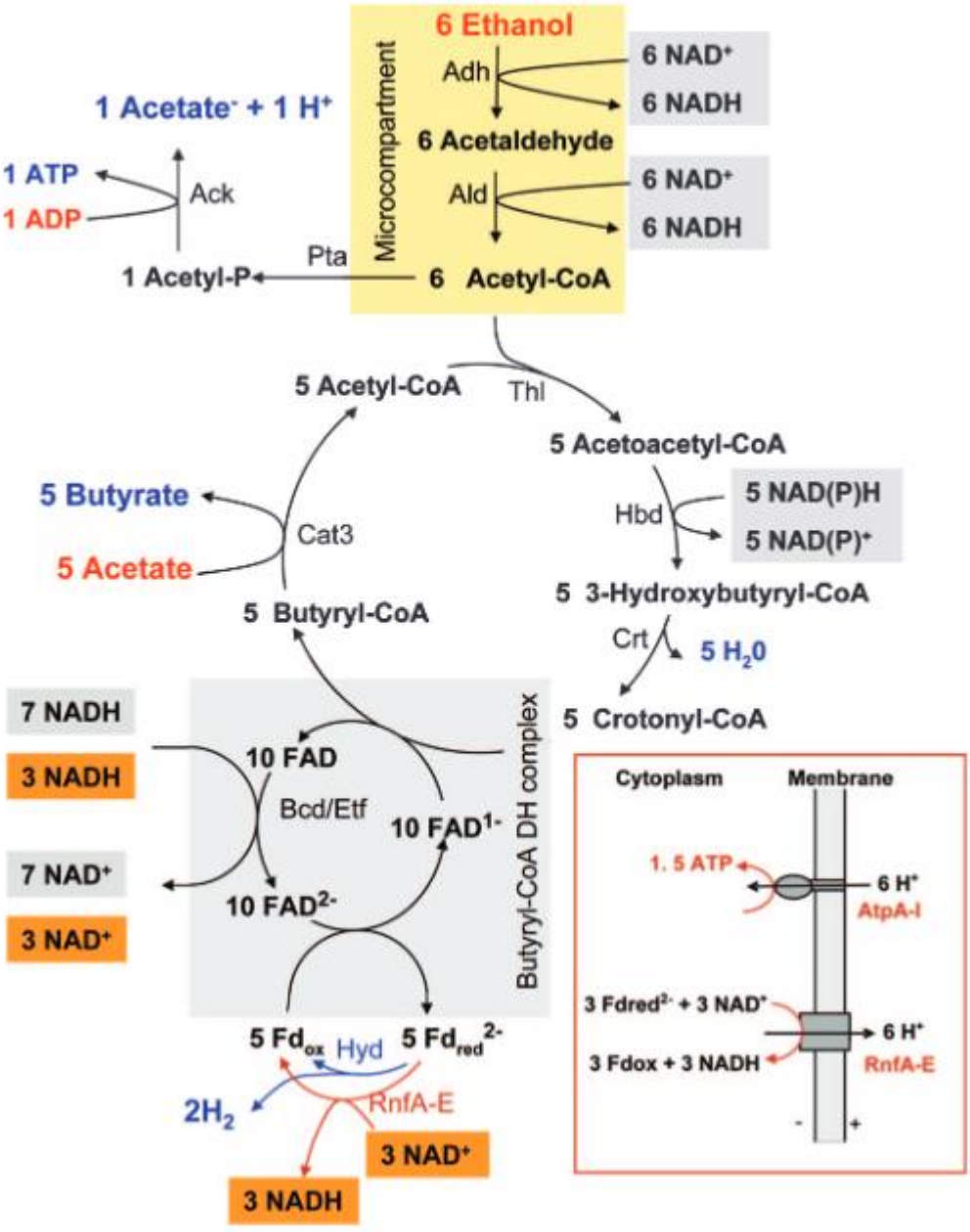
6 Ethanol
Microcompartment
Adh
6 NAD+
6 NADH
6 Acetaldehyde
Ald
6 NAD+
6 NADH
6 Acetyl-CoA
Pta
1 Acetyl-P
Ack
1 ATP
1 ADP
1 Acetate- + 1 H+
Thl
5 Acetyl-CoA
5 Acetoacetyl-CoA
Hbd
5 NAD(P)H
5 NAD(P)+
5 3-Hydroxybutyryl-CoA
Crt
5 H20
5 Crotonyl-CoA
Butyryl-CoA DH complex
10 FAD
Bcd/Etf
10 FAD1-
10 FAD2-
7 NADH
3 NADH
7 NAD+
3 NAD+
5 Butyrate
5 Acetate
Cat3
5 Butyryl-CoA
5 Fdox
Hyd
5 Fdred2-
2H2
RnfA-E
3 NAD+
3 NADH
Cytoplasm
Membrane
1. 5 ATP
6 H+
AtpA-I
3 Fdred2- + 3 NAD+
6 H+
3 Fdox + 3 NADH
RnfA-E
-
+

Figure.1.2. Illustration of metabolism of the *C. kluyveri*, including two membrane associated, energy-converting enzyme complexes involved in the fermentation: ferredoxin: NAD oxidoreductase (RnfA-E) and ATP synthase (AtpA-I). The clostridial ferredoxin with two [4Fe4S] clusters accept two electrons upon reduction . In the scheme it is assumed that 7 of the 10 NADH required for the reduction of 5 crotonyl-CoA to 5 butyryl-CoA are generated during ethanol oxidation to acetyl-CoA (gray background) and that three are generated via NAD+ reduction with Fdred2-(orange back-ground). It has been omitted that some of the Fdred2- generated during crotonyl-CoA reduction is also used for the regeneration of NADPH, which is required for acetoacetyl-CoA reduction. The yellow area indicates the micro-compartment, and the shaded area highlights the steps proposed to be involved in the catalysis by the butyryl-CoA dehydrogenase complex composed of butyryl-CoA dehydrogenase (Bcd) and the electron transport flavoproteins (EtfAB). Bcd, EtfA, and EtfB each contain FAD. Figure reproduced from Seedorf (2008)

1.1.4 *Clostridium saccharolyticum* and promising ethanol production

C. saccharolyticum is Gram-negative, ethanologenic bacterium.[10] Recently, *C. saccharolyticum* was renamed into *Lacrimispora saccharolytica*,[11] however, in the thesis this bacteria is still referred to as *C. saccharolyticum*. Like *C. acetobutylicum*, *C. saccharolyticum* metabolizes a variety of simple or complex sugars and produces a significant amount of ethanol but operates at a neutral pH.[10]Although studies about this species of *Clostridium* was not as extensive as the previous strains, *C. saccharolyticum* was reported to be producing ethanol and acetate.[3] It has great potential to be utilized in the syntrophic co-culture as an ethanol producer, which will be discussed in more detail in the later sections.

1.2 *Clostridium* syntrophic co-culture

Development of co-culture for bioprocessing avoids complicated engineering of a single species.[7] Instead, co-culture utilizes multiple species that work in both syntrophic and non-syntrophic manner to produce desired metabolites. In a review by Charubin *et al*, the pre-existing *Clostridium* co-culture applications to produce various proteins, alcohols, and acids has been thoroughly discussed.[7] Syntropy is defined as the combined metabolic activity of microorganisms, endergonic reactions can become exergonic through efficient removal of products and therefore enable a microbial community to survive with minimal energy resources.[12] This is especially important for many *Clostridium* co-culture designs, as they could produce and use a wide range of metabolites.

The syntrophic relationship between *C. ljungdahlii* and *C. acetobutylicum* was revealed by Charubin and Papoutsakis in a 2019 paper,[1] *C. acetobutylicum* upon catabolizing various carbohydrates, in addition to butanol, acetone, acetate and butyrate, it produces CO_2 and H_2 as byproducts of its metabolism. The co-culture between the two species can fix CO_2 (using H_2 as an electron donor) produced by the solventogenic *C. acetobutylicum* through the action of *C. ljungdahlii*, which utilizes CO_2 and H_2 for growth. This improves the carbon recovery (i.e., the fraction of substrate carbon converted into products, other than CO_2) in the co-culture fermentation. With 1.65 mol of H_2 2.25 mol of CO_2 produced per mol of sugar utilized in the *C. acetobutylicum* monoculture, and only 0.23 mol of H_2 and 0.73 mol of CO_2 produced per mol of sugar utilized in the *C. acetobutylicum* and *C. ljungdahlii* co-culture.[1] In addition, this co-culture produces 2,3-butanediol and isopropanol, which was not detected in the monoculture of either species. In this study, a model of direct cell-to-cell material exchange and the electron exchange between the two species was

proposed. Therefore, understanding to this cell-to-cell interaction between *C. ljungdahlii* and *C. acetobutylicum* would be critical to enhance the efficiency of *Clostridium* co-cultures.

The chain elongation metabolism of *C. kluyveri also* exhibits important traits for the *Clostridium* co-culture. *C. kluyveri* requires ethanol and acetate to perform chain elongation to produce longer change carboxylates. Ethanol and acetate are the metabolic products of *C. acetobutylicum, C. ljungdahlii* and *C. saccharolyticum*. The co-culture of these *Clostridium* species could yield a highly efficient fermentation process for high valued chemicals.[7]

1.3 Introduction of carbonic anhydrase (CA) and predicted CA localization in *C. ljungdahlii*

Carbonic anhydrases (enzyme code: EC 4.2.1.1) are metalloenzymes that catalyze the reaction of carbon dioxide hydration to bicarbonate and proton ($CO_2 + H_2O \leftrightarrow HCO_3^- + H^+$).[13] The activity of CA was suggested to be connected to bacteria survival, and high CA activity was demonstrated crucial in *Ralstonia eutropha* (a Gram negative facultative anaerobic bacteria) under a low CO_2 partial pressure environment.[13, 14] The enzyme can be classified into five genetically distinct families. In bacteria, three classes of CAs are known, the α-, β-, and γ-CAs.[13] Different classes of CAs are thought to localize differently in cells. The α-CA family of enzymes are found in Gram negative bacteria and is believed to be periplasmically localized and responsible for CO_2 fixation; β-, and γ-CAs are believed to be cytoplasmically localized and are responsible for CO_2 supplementation to the reactions catalyzed by carboxylase enzymes, for pH homeostasis and other intracellular functions.[15 16] In

Clostridium perfringens and *Clostridium autoethanogenum,* a β- CA was reported to be involved in cell metabolism.[17] [18] In *C. ljungdahlii, a* gene encoding a hypothetical CA was reported (CLJU_c10130). Since *C. ljungdahlii* is Gram positive, it is logical to speculate that the gene reported is a β- CA that likely localizes in the cytoplasm. Understanding the localization of CA enzyme in *C. ljungdahlii* might suggest how the organism utilizes the CA enzyme in CO_2 fixation and if the CA would show specific localization in the cells.

1.4 Introduction of methyl accepting chemotaxis protein (MCP) and MCP in *C. ljungdahlii*

The methyl accepting chemotaxis proteins (MCPs) are the most common chemotaxis receptors in prokaryotic and archaea species. MCPs are involved in mechanisms such as biofilm formation,[19] flagellum biosynthesis[20] and substrate detection and degradation[21]. MCPs are made up of a N-terminal module and a C-terminal module. The N-terminal module is responsible for stimulus detection that involves a ligand binding domain (LBD) and a transmembrane helix (TM). The C-terminal module includes a cytoplasmic signal (SD) domain responsible for downstream protein signaling. An example of the general structure is shown in Figure.1.3[22] [23]. The C-terminal module is similar across different MCPs while the N-terminal module is more diverse[22]. The detection mechanism of MCPs can be direct via ligand binding to LBD[24] or indirect via interactions between the ligand and a periplasmic binding protein[25]. Lacal et.al. have classified MCPs into 7 classes based on different domain structures and topological interactions between the protein and the cell membrane. The most common structure is Class I[26] and is depicted in Figure.1.3. The localization of MCPs varies between different organisms and even different

MCPs within one organism can localize differently. Most bacterial transmembrane MCPs localize to the polar ends of the cells, although, in *Pseudomonas aeruginosa*, lateral localization was reported for the WspA receptor protein, which is bioinformatically indistinguishable from MCPs [27]. *Bacillus subtilis,* a Gram positive facultative anaerobe bacterium, was reported to have polar localization of MCPs. *E.coli,* a Gram negative facultative anaerobe was reported to have polar MCP clusters and random insertion of lateral MCPs[28] (Figure.1.4). MCPs were reported to be essential for the survival of many prokaryotes and archaea. Many gene coding for uncharacterized MCPs are annotated in *C. ljungdahlii* genome. The MCP (CLJU_c10160) selected for this study is located near the gene for CA and flagellar machinery. Therefore, it was hypothesized to be more likely to be involved in the CO_2 sensory mechanism. Additionally, as there has not been a reported CO_2 receptor for this organism, testing this uncharacterized MCP that is near an enzyme for CO_2 metabolism may provide insights into prokaryotic CO_2 sensory mechanisms. Understanding the role of MCPs can elucidate how an organism recognizes and interacts with the environment, which can help reveal the role of MCPs in the direct cell-to-cell material exchange phenomenon between *C. acetobutylicum* and *C. ljungdahlii*[29].

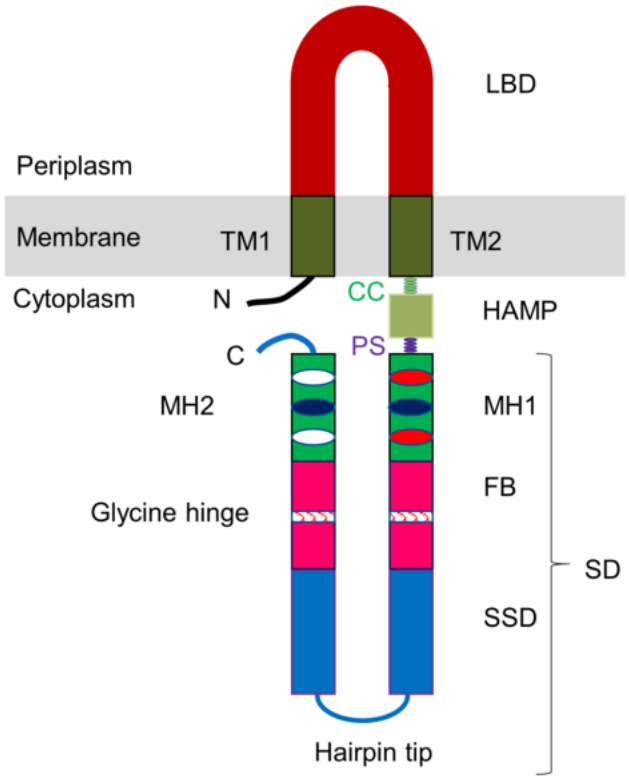

Figure.1.3. Overall topology of typical methyl-accepting chemotaxis protein. LBD ligand binding domain, TM transmembrane helix, CC control cable, HAMP histidine kinase, adenyl cyclase, methyl-accepting chemotaxis protein and phosphatase region, PS phase stutter, SD signaling domain, MH methylation helix, FB flexible bundle, SSD signaling subdomain. Reproduced from Salah et.al (2017).

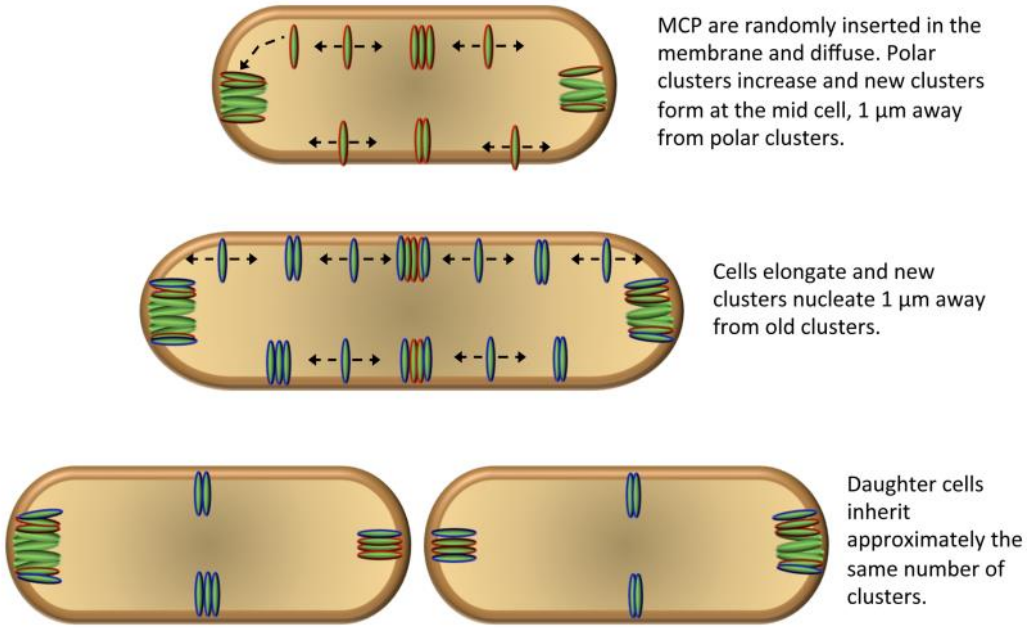

Figure.1.4. Schematic representation of the stochastic self-assembly model proposed by Thiem and Sourjik (2008)30for the *E. coli* MCP cluster formation. Reproduced from Emilia et.al (2018)[28].

1.5 Anaerobic reporting system and anaerobic fluorescent proteins

Genetic reporters are genes that provide measurement and screening of gene expression. As described in a review by Joseph and colleagues, an ideal reporter system has high sensitivity and specificity, a large dynamic range of detection, and low level of endogenous level of the reporter in the strain of interest[31]. For *Clostridium* species typical reporter systems include enzymatic reporters and bioluminescent reporters[31]. However, fluorescent reporters were not widely used as the common strong fluorescent reporters such as green fluorescent protein (GFP) and mCherry require O_2 activation.[32 33] This is not possible for strictly anaerobic organisms. Anaerobic fluorescent proteins enable an array of applications including screening of proteins, genomic and metagenomic libraries, study of promoters, ribosomal-binding sites and terminators, and study of microbiome interactions, as well as creating fluorescent fusion proteins to study the localization of proteins in cells[34]. Utilizing fluorescent proteins would allow real-time analysis of protein expression and cell interaction under flow cytometry and microscopy. Recently Charubin *et al* and Streett *et al* created a strong fluorescent protein designed for anaerobic species, that requires only ligand binding to be fluorescent and no O_2 activation is required. The proteins are Fluorescence-Activating and Absorption-Shifting Tag (FAST)[35], Halotag, and SNAP-tag.[34] Among those, FAST has successfully shown to fluoresce when fused with a cell division protein ZapA in *C. ljungdahlii*[35].

Chapter 2

Optimization of *Clostridium* dual culture bioreactor performance

2.1 Introduction

As mentioned in Chapter 1, the traditional ABE fermentation utilizing *C. acetobutylicum* monoculture is economically challenged, as acetone and butanol can be produced more cheaply via petrochemical route. With recent developments in genetic engineering tools, the metabolism of bacteria can be engineered to yield desired products. Sillers et.al. had made progress in creating a higher solvent producing *C. acetobutylicum* strain containing the pCASAAD plasmid, namely the *Cac*(pCASAAD) strain[36]. The *Cac*(pCASAAD) strain overexpress the native alcohol/aldehyde dehydrogenase (AAD) enzyme, an enzyme that converts butyryl-CoA to butanol or acetyl-CoA to ethanol, using the *ptb* promoter, which is an active promoter during the acidogenic phase of *C. acetobutylicum*[36 37 38]. The *Cac*(pCASAAD) strain was reported to produce 30 g/L of solvents mainly consist of ethanol and butanol, compare to wildtype only 20 g/L of solvent was produced and mainly consist of acetone and butanol[36]. This progress had strengthened the economic argument of utilizing engineered *C. acetobutylicum* for a solvent production process, to overcome bottlenecks and maximize the production of desired metabolites. However, improved ethanol and butanol production might not be potent enough for industry to convert back to ABE fermentation, thus production of higher valued chemicals are desired. It is known that engineering new pathway into bacteria remains challenging, therefore, incorporating new species of bacteria and allowing each species to specialize on a task would be more realistic. For the rest of this chapter *Cac*(pCASAAD) is referred as *C. acetobutylicum.*

As previously mentioned, medium/ long chain alcohol and fatty acid are high value chemicals that can be produced by ethanol and acetate consuming *C. kluyveri*. Co-culturing the high ethanol producing *Cac*(pCASAAD) strain with *C. kluyveri* could yield valuable medium/long chain alcohol and fatty acid products, thus bringing more industrial significance. In addition, *C. acetobutylicum* like all organisms releases at least one-third of the carbons in six-carbon sugars in form of CO_2 due to the pyruvate to acetyl-CoA decarboxylation reaction, whereby, for anaerobes at least, the electrons from the decarboxylation reactions are used to form and release H_2. Acetyl-CoA is the starting intermediate for the biosynthesis of most metabolites like butanol, acetone, ethanol, butyrate and acetate. Recovering these CO_2 molecules could be solved (to the extent that are available electrons such as in the form of H_2) by introducing a CO_2-fixing acetogen, such as *C. ljungdahlii,* into the culture. Achieving complete carbon utilization in the system will increase the yield for acetate which could be potentially converted to higher value chemicals by *C. acetobutylicum*. In the proposed co-culture, *C. acetobutylicum* consumes glucose and produce ethanol and acetate for *C. kluyveri* to produce long chain fatty acids, and then *C. acetobutylicum* can convert fatty acids into their corresponding alcohols using an aldehyde and alcohol dehydrogenases to recover NAD^+ from NADH[39]. In addition *C. saccharolyticum* can also consume sugar and produce ethanol and acetate however this strain lacks the ability to convert carboxylates into alcohol. For the scope of this thesis, the focus is on improving the economically significant medium/long chain alcohol production in a *Clostridium* dual culture design and investigating the effect of bioreactor conditions on the product yield and substrate utilization.

In a study by Lonkar et al, the optimal fatty acid conversion of *C. kluyveri* occurs at an ethanol concentration of 5-10 g/L, which produced around 80 mM of hexanoate. Ethanol toxicity to *C. kluyveri* is significant at a concentration above 40 g/L. Additionally, in the paper, the pH was maintained at 6.8 to 7.0 in order to reduce their inhibitory effect on *C. kluyveri*.[40] In a separate study of *C. acetobutylicum* by Roos et al, at pH above 6.0, *C. acetobutylicum* expresses an autolysin that results in significant cell lysis and cell death[4]. The pH incompatibility of *C. acetobutylicum* and *C. kluyveri* co-culture would suggest a limitation on growth and productivity for a co-culture of the two species. Thus, investigation of another solventogenic strain with an optimal pH between 7.2 and 7.4[10], *C. saccharolyticum,* suggests that it has a good potential in the co-culture to substitute for *C. acetobutylicum* as the ethanol- and acetate-producing strain. This investigation would aid future studies of *Clostridium* co-cultures that yield high-value alcohol products and improve the recovery of carbon waste (CO_2).

2.2 Material and Methods

2.2.1 Bacterial strains, Media, Bioreactors, and Analytical tools

All strains used are shown in Table.A.1 of Appendix.A. The *C. acetobutylicum* *Cac*(pCASAAD)[36] strain used was grown on solid 2xYTG medium (16 g/L tryptone, 10 g/L yeast extract, 4 g/L NaCl, 5 g/L glucose, and 15 g/L agar [pH 5.8]), and Turbo Clostridium Growth Medium (CGM)[1]. The plated *C. acetobutylicum* were grown on 2xYTG plate for at least five days before colonies were inoculated in 10 mL Turbo CGM (80 g/L glucose) with 200 µL of phosphate buffer (100 g/L of KH_2PO_4 and 125 g/L K_2HPO_4 [pH 6.8]). The tubes were then heat shocked for 8 minutes at 80°C, and

after cooling, erythromycin was added to 100 ug/mL. *C. kluyveri* was grown in liquid Turbo CGM (no glucose, with 8 g/L sodium acetate). One 1 mL tube of glycerol stock was thawed and inoculated in 90mL of medium (additional 1 mL of phosphate buffer, 1 mL of 3% weight to volume ratio L-cysteine HCl solution, 2mL of pure ethanol, and 2.7 mL of 10% weight to volume ratio sodium bicarbonate solution) and was grown for five days, then 5mL of the starting *C. kluyveri* culture was passaged into the same Turbo CGM for active growth overnight. *C. saccharolyticum* was inoculated from 1 ml of glycerol stock into 90mL of Turbo CGM (80 g/L glucose, with an additional 1mL phosphate buffer and 2.7 mL of 10% weight to volume ratio sodium bicarbonate solution) overnight. All cell cultures described above were incubated within an anaerobic chamber filled with 5% H_2, 15%CO_2, and 80%N_2 gas mix at 37ºC without any other external interruption overnight or up to 16 hours.

Also, a set of self-constructed miniature bioreactors was employed for *C. saccharolyticum* and *C. kluyveri* fermentation. The miniature bioreactors had functions of automatic pH adjustment, agitation, gas sparging, and sampling. This vessel could operate with 180-200mL active volume, and in all subsequent fermentation utilizing the miniature bioreactors, 180mL of volume was used.

Optical density was determined at a wavelength of 600 nm (OD_{600}) using a Beckman-Coulter DU370 spectrometer. The OD_{600} was used to estimate the cell density within the bioreactor.

High Performance Liquid Chromatography (Agilent 1200 series) with Aminex HPX-87H column was used to analyze the concentration of the metabolites.

2.2.2 Inoculation and fermentation strategy for bioreactor experiments

The solventogenic *C. acetobutylicum* and ethanologenic *C. saccharolyticum*, were inoculated by injecting 10 mL overnight cell culture from the anaerobic incubator into the bioreactor. *C. kluyveri* was inoculated via centrifuging the overnight culture in 50mL conical tubes at 4000 rpm for 8 minutes and collecting the cell pellet, then injecting the resuspended cell pellets into the bioreactor.

For co-culture experiments, solventogenic bacteria were inoculated into the bioreactor before *C. kluyveri. C. acetobutylicum* cells were left in the bioreactor for 8-16 hours to accumulate ethanol. *C. saccharolyticum* cells were left to grow for 8-16 hours to accumulate ethanol. The concentration of the desirable chemicals was monitored via HPLC.

A typical bioreactor experiment was kept running for 48-72 hours, until the cells exhausted all available nutrients and were not producing more products.

2.3 Results and Discussion

2.3.1 *C. kluyveri* monoculture pH range suggests that *C. acetobutylicum* and *C. kluyveri* co-culture displays incompatible optimal pH

As previously mentioned, the optimal pH for the two strains of bacteria in the initial design is incompatible. Thus, if the culture pH overly favors one species, the environment is harmful to the other one, which affects its growth and metabolism. Therefore, monoculture experiments were conducted at various pH levels to investigate possible feasible pH setpoints for *C. acetobutylicum* and *C. kluyveri* co-culture.

C. kluyveri monocultures were set up in 7 separate 100 mL bottles, without any replica, which were incubated with the same methodology as the passaged *C. kluyveri*

cultures. The pH of the monocultures was initially adjusted using 1M NaOH solution in a range of pH 5.0 to 6.25 with 0.25 increments, and one culture was left without any initial pH adjustment (Normal) so the Turbo CGM media pH is shown. No further pH control was given to the cultures. The results are shown in Figure 2.3.1. As shown below, the culture without initial pH adjustment stabilized to pH 6.6 (Figure 2.3.1.B). This control culture of *C. kluyveri* displayed a higher growth rate, ethanol and acetate consumption, and metabolite production (28 mM of butyrate, in Figure 2.3.1.E, and 80 mM of hexanoate, in Figure 2.3.1.F, after 120 hours) compared to all other cultures with lower initial pH levels. Although not as efficient as the normal culture, the *C. kluyveri* culture at pH 6 and 6.25, produced significant amounts of butyrate (36 mM and 35 mM respectively), but hexanoate production was affected as the concentration only reached 40 mM and 30 mM after 120 hours of culture. The monoculture at pH 5.75 started to produce butyrate and hexanoate after 60 hours of incubation, however the yield after 120 hours was not sufficiently high (butyrate 26 mM and hexanoate 9.5 mM). Because ethanol is used for sterilization in the anaerobic chamber, ethanol is enriched in the chamber atmosphere. In Figure 2.3.1.D, the increase in ethanol concentration over time is due to the ethanol in the chamber atmosphere. The other monocultures at lower pH showed little to no active metabolism or chain elongation.

Based on the previous experiments, there is only a narrow pH range (pH 5.75-pH 6) for the co-culture of *C. acetobutylicum* and *C. kluyveri* to be feasible. However, within this narrow pH range, *C. kluyveri* displayed delayed and limited activity with low hexanoate production. Therefore, *C. saccharolyticum* and *C. kluyveri* co-cultured were explored next. Before pursuing *C. saccharolyticum* and *C. kluyveri* co-cultures,

production of hexanoate from *C. kluyveri* monoculture under optimized conditions was pursued further.

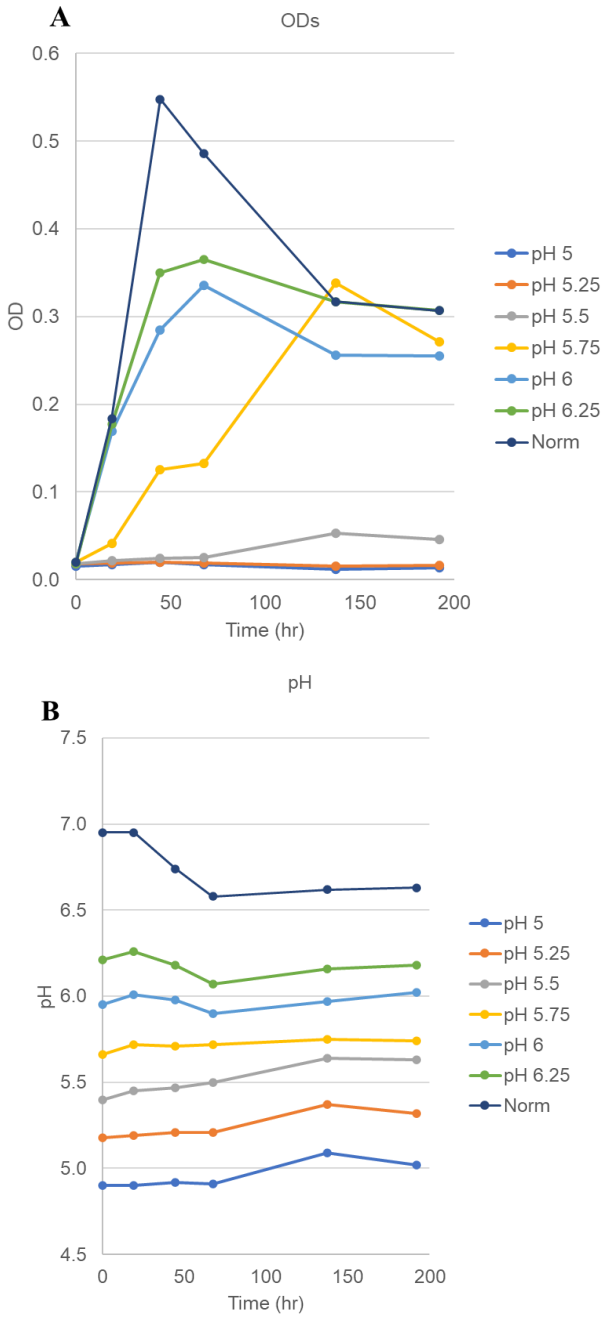

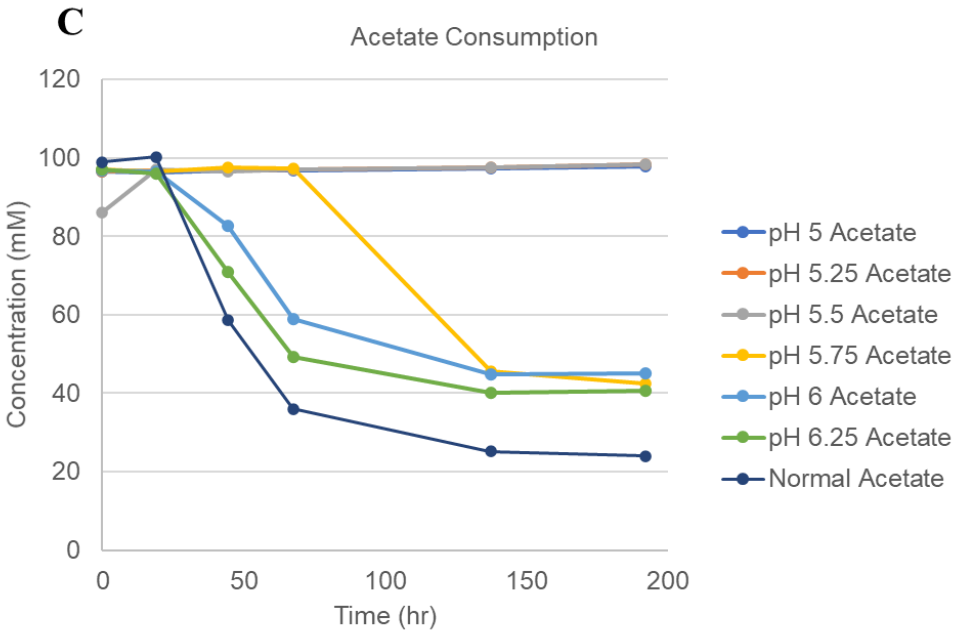
C
Acetate Consumption
120
100
80
60
40
20
0
Concentration (mM)
0
50
100
150
200
Time (hr)
pH 5 Acetate
pH 5.25 Acetate
pH 5.5 Acetate
pH 5.75 Acetate
pH 6 Acetate
pH 6.25 Acetate
Normal Acetate

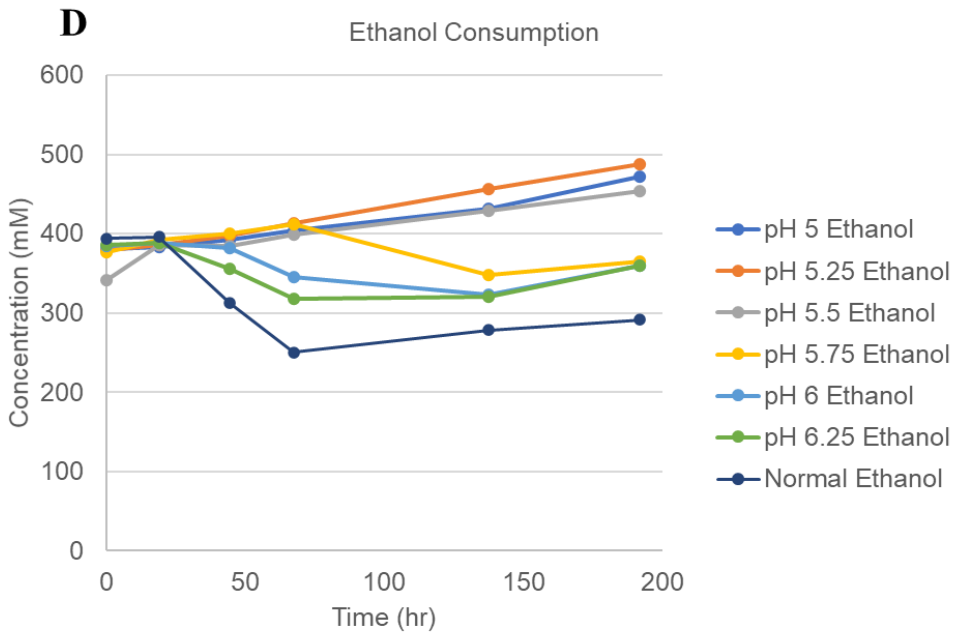
D
Ethanol Consumption
600
500
400
300
200
100
0
Concentration (mM)
0
50
100
150
200
Time (hr)
pH 5 Ethanol
pH 5.25 Ethanol
pH 5.5 Ethanol
pH 5.75 Ethanol
pH 6 Ethanol
pH 6.25 Ethanol
Normal Ethanol

E

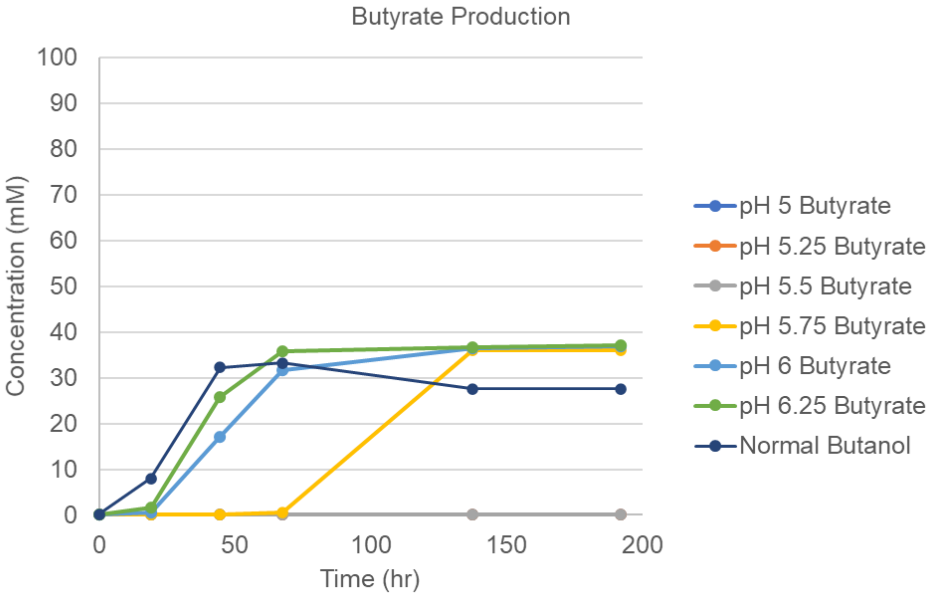
Butyrate Production
Concentration (mM)
Time (hr)
0
10
20
30
40
50
60
70
80
90
100
0
50
100
150
200
pH 5 Butyrate
pH 5.25 Butyrate
pH 5.5 Butyrate
pH 5.75 Butyrate
pH 6 Butyrate
pH 6.25 Butyrate
Normal Butanol

F

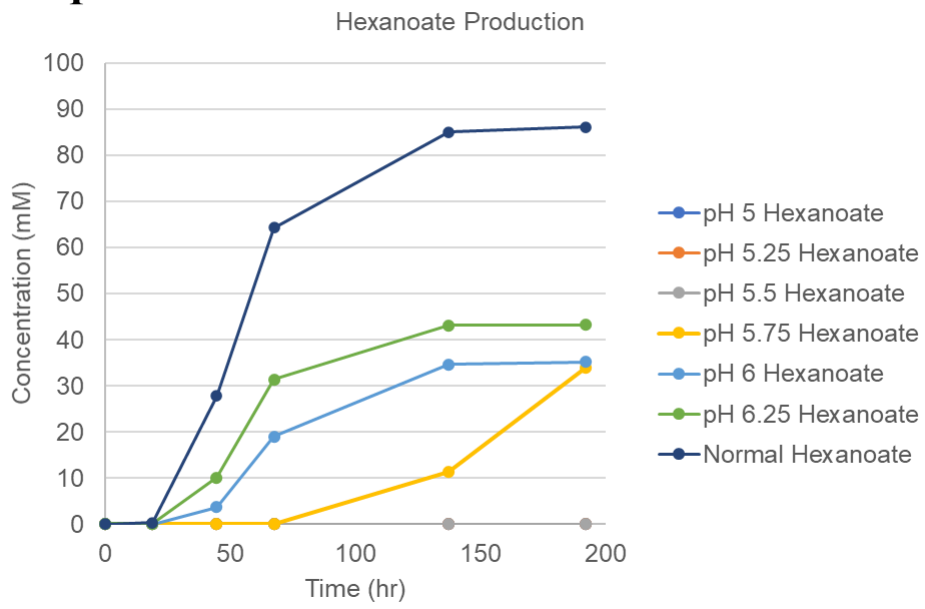
Hexanoate Production
Concentration (mM)
Time (hr)
0
10
20
30
40
50
60
70
80
90
100
0
50
100
150
200
pH 5 Hexanoate
pH 5.25 Hexanoate
pH 5.5 Hexanoate
pH 5.75 Hexanoate
pH 6 Hexanoate
pH 6.25 Hexanoate
Normal Hexanoate

Figure.2.3.1. *C. kluyveri* monoculture under various pH levels. Normal indicates monoculture without pH adjustments. (n=1) No replicates were made. **A**. monoculture OD600 variation. **B**. monoculture pH variation. **C**. acetate consumption. **D**. ethanol consumption. **E**. butyrate production. **F**. hexanoate production

As shown in Figure 2.3.1, without pH control simple batch monocultures of *C. kluyveri* produced about 80 mM of hexanoate, which is close to the best hexanoate production reported in many previous studies of *C. kluyveri*[9, 40]. To further explore the biosynthetic capabilities of *C. kluyveri* for hexanoate production prior to its use in co-cultures, optimization of *C. kluyveri* monocultures was further pursued using the small bioreactors.

Four monocultures were conducted in parallel with an active volume of 180 mL. The pH was automatically controlled at around pH 7. *C. kluyveri* from the same glycerol stock was grown and passaged as described in the method section, and then the prepared *C. kluyveri* was inoculated into the bioreactor for a starting OD level of 0.7. The results are shown in Figure 2.3.2. The pH control and OD change of the monoculture can be seen in Figure 2.3.2A. *C. kluyveri* reaches the stationary phase after 24 hours of fermentation but hexanoate accumulation continues. The ethanol concentration was maintained above 250 mM, and acetate concentration was maintained above 50 mM as shown in Figure 2.3.2B. At hours 6, 17, and 36, additional ethanol and acetate were supplied, indicated by a sharp increase of both concentrations on the graph. In Figure 2.3.2C shows the concentration profiles of the produced butyrate and hexanoate. Butyrate concentration was maintained relatively constant and increased above 50 mM. The low butyrate accumulation is due to the

active chain elongation reaction in *C. kluyveri* which uses butyrate as an intermediate building block to form hexanoate[40]. This leads to a high hexanoate concentration of about 180 mM within 45 hours of fermentation, doubling the previously reported hexanoate production[40]. Octanoate could not be efficiently detected via the current HPLC and it is not the product of interest for this project thus the octanoate concentration was not shown in the data.

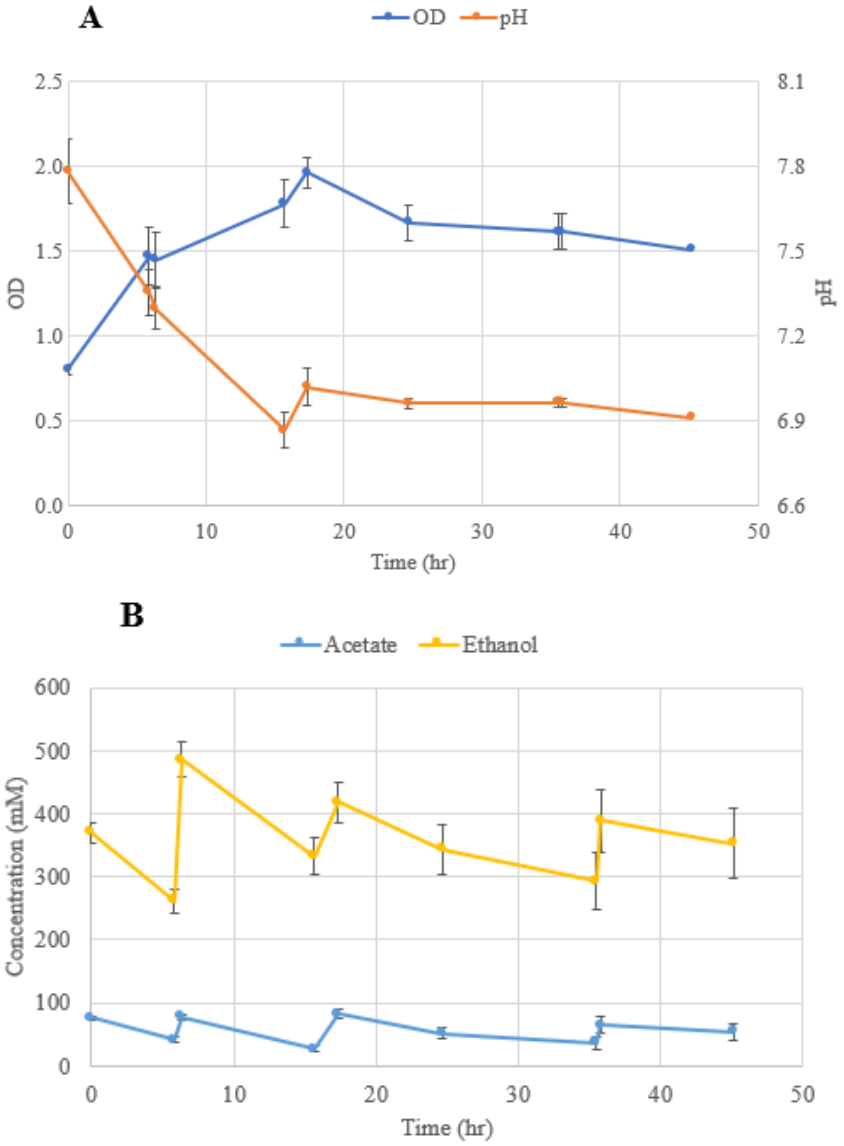

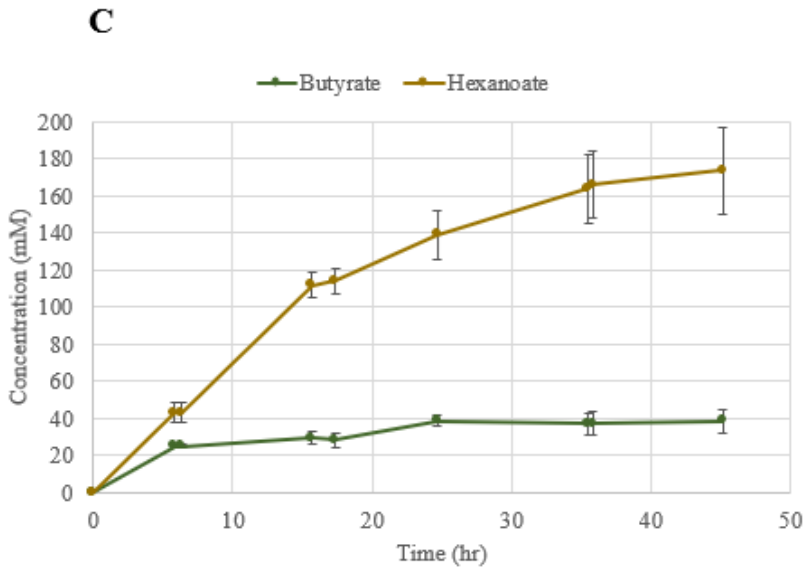

Figure.2.3.2. *C.kluyveri* monoculture miniature bioreactor with pH monitoring and control and constant stirring (n=4) **A.** pH and OD variation **B.** Nutrient (ethanol and acetate) consumption **C.** Product (butyrate and hexanoate) accumulation

The *C. kluyveri* monoculture exhibits the capacity of the bacteria for high hexanoate accumulation within two days of fermentation under an ideal growth condition with pH control and an abundance of nutrients. The *C. kluyveri* monoculture experiment had set an upper boundary of hexanoate production to compare the co-culture performance. In the co-culture, the ethanol concentration would not be as abundant as in the monoculture, therefore a reduction in the hexanoate production was expected.

2.3.2 *C. saccharolyticum* and *C. kluyveri* co-culture yield abundant hexanoate production

Fermentation using ethanol and acetate as feed to generate hexanoate is economically challenged. Therefore, utilizing glucose-consuming and solvent-producing bacteria to supply substrate for *C. kluyveri* would bring more industrial significance as the unit price for glucose is typically lower than solvents. As previously shown, the high hexanoate productivity of *C. kluyveri* can be achieved at neutral pH and high ethanol concentrations.

Two co-cultures were run in parallel in the miniature bioreactor with an active volume of 180mL. The pH in the bioreactor was controlled to around 7.0 and the OD variation can be seen in Figure.2.3.3.A. *C. saccharolyticum* was inoculated at 0.2 OD in the bioreactor and was grown until ethanol concentration reached 148mM (16 hours) and OD level reached 4.5. At 16 hours *C. kluyveri* was inoculated and an 0.5 OD increase could be observed in the bioreactor. The more abundant *C. saccharolyticum* cell density provided more ethanol for *C. kluyveri* to utilize. As seen in Figure.2.3.3.B, the glucose concentration was maintained above 200 mM by glucose addition at 16, 23, 29, and 38 hours. In Figure.2.3.3.C, after *C. kluyveri* inoculation, the ethanol concentration was quickly depleted as *C. kluyveri* cells consumed ethanol to produce hexanoate. In the co-culture, 8 hours after *C. kluyveri* inoculation, 55 mM of hexanoate was produced. In the monoculture 6 hours after *C. kluyveri* inoculation, 46mM of hexanoate was produced, see Figure.2.3.2.C. As the co-culture fermentation continues, before 40 hours (24 hours since *C. kluyveri* inoculation) *C. saccharolyticum* maintained a steady glucose consumption rate, Figure.2.3.3.B, and ethanol production rate, Figure.2.3.3.C. However, *C. kluyveri* consumed more ethanol than *C. saccharolyticum* produced in the co-culture, so the

ethanol concentration in the culture quickly depleted to around 20mM. At lower ethanol concentration, the performance of the chain elongation reaction of *C. kluyveri* was impeded, which was shown by the slowed hexanoate accumulation, shown in Figure.2.3.3.C. At 70 hours (54 hours since *C. kluyveri* inoculation), hexanoate concentration reached 123 mM. At 77 hours, hexanoate concentration was 124mM, as it plateaus as the ethanol concentration dropped below 20 mM, indicating minimal activity from both bacteria in the co-culture three days into the co-culture experiment. Throughout the fermentation, butyrate concentration was stable at around 40 mM, as butyrate was converted into hexanoate via chain elongation reaction of *C. kluyveri* during the fermentation.

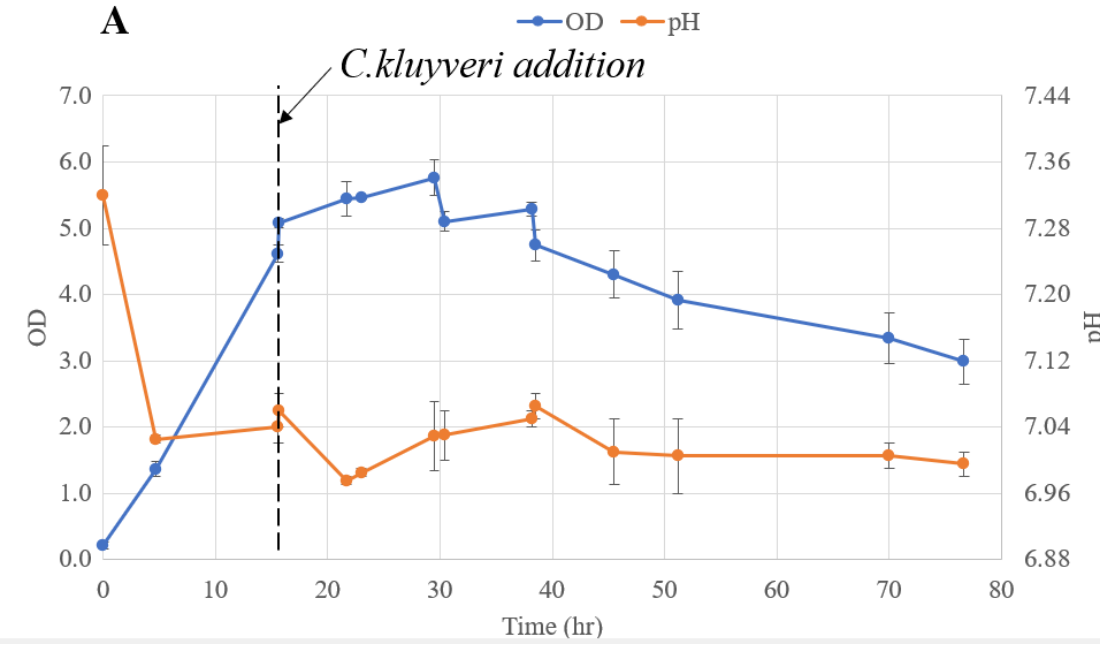

B

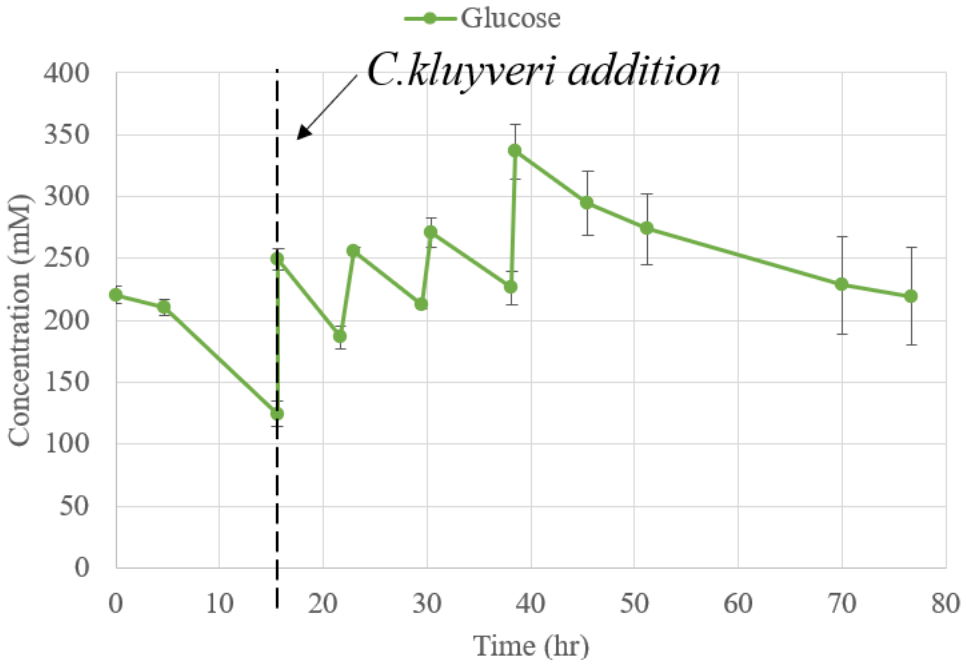
Glucose
C.kluyveri addition
Concentration (mM)
Time (hr)
0
50
100
150
200
250
300
350
400
0
10
20
30
40
50
60
70
80

C

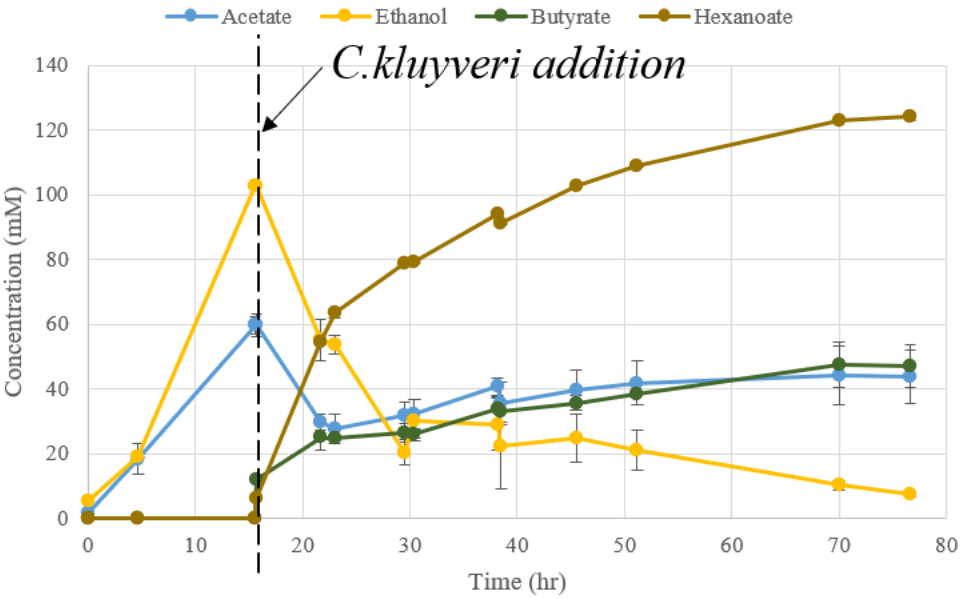
Acetate
Ethanol
Butyrate
Hexanoate
C.kluyveri addition
Concentration (mM)
Time (hr)
0
20
40
60
80
100
120
140
0
10
20
30
40
50
60
70
80

Figure.2.3.3. *C. kluyveri* - *C. saccharolyticum* co-culture in the miniature bioreactor with pH control and monitoring (n=2). **A.** pH and OD variation **B.** Nutrient (glucose) consumption **C.** Product (ethanol, acetate, butyrate, and hexanoate) accumulation. Error bars were taken as standard error.

2.4 Discussion and conclusion

From the initial monoculture experiments, the pH incompatibility between *C. acetobutylicum* and *C. kluyveri* was demonstrated. Low pH causes a significant interruption to the activity of *C. kluyveri*, because when a culture was started at pH 5.75, the cells experienced a 68 hour delay and only reached a final hexanoate concentration of 35 mM. For cultures with starting pH of 6 and 6.25, limited hexanoate production was observed compared to the monoculture started at pH around 7 (Figure 2.3.1.F). Since *C. acetobutylicum* cell lysis was reported above pH 6[4], the *C. acetobutylicum* and *C. kluyveri* co-culture performance would be greatly impeded by the pH incompatibility between bacteria. The optimized *C. kluyveri* monoculture experiment demonstrated the capacity of this organism to produce 180 mM of hexanoate when fed high ethanol concentrations with a high ethanol to acetate ratio (Figure 2.3.2. C). The monoculture experiment exhibited unprecedented hexanoate production from *C. kluyveri* and set the goal for subsequent co-culture experiments with *C. kluyveri*.

The *C. saccharolyticum* and *C. kluyveri* co-culture yielded promising results as they achieved higher hexanoate concentration than all other previously reported studies[40] (123 mM within 70 hours of overall fermentation time, Figure 2.3.3.C). Still, the co-culture hexanoate production was 60 mM less than at the *C. kluyveri*

monoculture, indicating further improves to the co-culture system is possible. The hexanoate productivity seems correlated with the ethanol concentration, as shown in Figure 2.3.3.C. In co-culture, high ethanol concentrations (between 138mM to 54 mM) were maintained in the first 6 hours after *C. kluyveri* inoculation. Thus, in the first 6 hours the co-culture hexanoate production (48 mM of hexanoate) is comparable to *C. kluyveri* monoculture experiment (43 mM of hexanoate). As the initially accumulated ethanol was consumed, ethanol productivity of *C. saccharolyticum* limited the performance of *C. kluyveri* as demonstrated by the reduced hexanoate productivity. Even though the hexanoate production of this co-culture was not as high as in the monoculture, the co-culture still seems economically more promising than the monoculture as the glucose feed of the co-culture is much cheaper than the ethanol and acetate feed required by the monoculture. Furthermore, *C. saccharolyticum* also produces CO_2 and H_2 gas[10], and *C.kluyveri* has been reported utilize CO_2 for growth, so co-culture might enhance the hexanoate productivity[41]. Therefore, with enough ethanol supplied to *C.kluyveri* the co-culture hexanoate productivity might be further enhanced from the monoculture due to the CO_2 availability to *C.kluyveri* in the co-culture. The ethanol productivity could be improved by inoculating the *C.saccharolyticum* at a higher OD to achieve higher ethanol production and adding fresh *C.saccharolyticum* cells into the bioreactor a few hours after the inoculation of *C.kluyveri* to maintain a high ethanol productivity in the co-culture. Also, modifying the bioreactor system by growing *C.saccharolyticum* in the first reactor and supplying fresh medium, allowing the cells to accumulate ethanol. And *C.saccharolyticum* culture can be continuously moved to the second reactor for co-culture with *C.kluyveri*. Designing a system of serial continuous bioreactor might improve the

performance of the co-culture and will bring more industrial insights to the co-culture fermentation. In addition, *C. ljungdahlii* could be introduced to the co-culture for CO_2 recovery and produce more ethanol and acetate as substrate for *C. kluyveri* for hexanoate production. Also, *C. ljungdahlii* can convert the fatty acids produced into their corresponding alcohols[2], which will produce more products such as butanol and hexanol. Therefore, the *C. saccharolyticum* and *C. kluyveri* binary co-culture exhibit a promising alternative for the *Clostridium* syntropic co-culture design, and the possible feasibility of incorporating *C. ljungdahlii* into the co-culture to promote its performance and reduce carbon waste.

Chapter 3

Use of fluorescent fusion protein to probe heterologous cell fusion events

3.1 Introduction

As described in Chapter 1 of the thesis, a robust and reliable reporter system is important in the study of co-culture phenotype, and a reporter system utilizing fluorescent protein would also enable studies of protein localization, and real-time analysis of bacteria culture using flow cytometry and microscopy. In the lab, Charubin and Streett have developed strong anaerobic fluorescent proteins Halotag and FAST. These anaerobic fluorescent proteins are highly expressed utilizing phosphotransacetylase gene promoters[34 35, 36]. Previously, the anaerobic fluorescent fusion protein was successfully constructed on a cell division protein ZapA tagged with FAST, and the protein localization was also probed[35]. Halotag works in a similar fashion as FAST, however, Halotag fluorescence can be expressed by forming a covalent alkyl-enzyme bond with the ligand[42]. Proteins that are tagged with Halotag have not been reported, so to determine the feasibility of observing protein localization using Halotag fused protein was conducted. Using fluorescent reporter systems can help establish cellular interaction and phenotypes that could be further probed.

As mentioned previously, the direct cell-to-cell material exchange between *C. acetobutylicum* and *C. ljungdahlii* was observed. This allowed the exchange of cytoplasmic materials and improved the CO_2 fixation of the acetogen, and inhibition of cell contact causes a significant drop in CO_2 utilization in *C. ljungdahlii*[1, 7]. However, the mechanism of the cell fusion events is unclear. It is important to understand this mechanism to yield a better understanding of how *C. ljungdahlii* seeks out nutrients and to engineer a more efficient *Clostridium* coculture. This fusion event may be

involved with a CO_2 sensing mechanism in *C. ljungdahlii* via chemotactic sensing. The associated chemotaxis is the mechanism by which microorganisms sense chemicals and move towards beneficial and away from unfavorable environments[23].

As mentioned in the previous chapter, the methyl accepting chemotaxis proteins (MCPs) are the most common receptors in prokaryotic and archaea species[23], and a section of *C. ljungdahlii* genome was predicted to be MCP in Kyoto Encyclopedia of Genes and Genomes (KEGG) database. However, no studies were conducted to investigate the MCP in *C. ljungdahlii*. The MCP classification, localization, and functionality in *C. ljungdahlii* are unclear. We hypothesized that MCP is the chemoreceptor that aids *C. ljungdahlii* to detect attractant such as CO_2 thus promote cell-to-cell direct material exchange between the *C. acetobutylicum* and *C. ljungdahlii*. To test the hypothesis, MCP must be better understood, protein localization study can reveal if the predicted MCP in *C. ljungdahlii* is a transmembrane protein and possess similar polar or lateral localization behavior as previously reported[27, 43].

Also, there are multiple enzymes that may assist cells to metabolize CO_2 such as carbonic anhydrase (CA) that converts CO_2 into bicarbonate in many bacteria species including *C. ljungdahlii*. These proteins may aggregate at the CO_2 rich end of the cell[13]. The fluorescent fused protein of CA and MCP could be potential tools for *C. acetobutylicum* and *C. ljungdahlii* co-culture studies to reveal the sensory and cell fusion mechanism of *C. ljungdahlii* to *C. acetobutylicum*. In this thesis, construction of the fluorescent fusion proteins and preliminary screening of their localization was conducted, which provides the foundation for future co-culture studies with fluorescent fused proteins.

3.2 Methods

3.2.1 Chemicals

E. coli NEB 5-α, E. coli NEB 10-β, Q5 DNA polymerase, Phusion DNA polymerase, and NEBuilder HiFi DNA assembly master mix were purchased from NEB (Ipswich, MA). Also, Phusion High Fidelity DNA polymerase and Phire Hot Start II DNA polymerase were purchased from Thermo Fisher Scientific (Waltham, MA). Restriction endonucleases were purchased from Thermo Fisher Scientific (Waltham, MA). The fluorescent ligands used were commercially available ^{TF}Lime (The Twinkle Factory, France), TMR Direct Halotag and Jenalia 646 (Promega).

3.2.2 Bacterial strains, Media and Growth Conditions

All strains and plasmids used are listed in Appendix A, Table.A-1. Plasmids' propagations were conducted in chemically competent E. coli NEB 5-α strain, the plasmid was methylated in 10-β strain for transformation into *C. ljungdahlii*. *E. coli* were grown under 37 °C at 250 rpm in a liquid LB media or without rotation on a solid LB agar plate. LB media includes 10 g/L NaCl, Bacto Trytone 10 g/L, yeast extract 5 g/L, and 15 g/L agar if solid plates are made. *C. ljungdahlii* is grown in ATCC 1754 medium with no glucose and 5 g/L fructose Or Turbo CGM medium. To plate the transformed *C. ljungdahlii*, molten Reinforced Clostridia Media (RCM) (Fisher Scientific) was used with 8 g/L agar added.

C. ljungdahlii wildtype and transformed strains were inoculated into 160 mL serum bottle containing 20 mL of Turbo CGM media (5 g/L fructose) and was applied a 20 psi overhead pressure of 887 gas mix (20% CO_2 and 80% H_2) unless specified otherwise. OD_{600} was measured to monitor the growth of the bacteria using Beckman-Coulter DU370 spectrophotometer.

3.2.3 Plasmid design and construction

The plasmid was designed to obtain a strong expression of the fluorescent fused protein in the targeted bacteria strain. The plasmid was constructed to contain ampicillin resistance (AmpR), Erythromycin resistance (ErmR), phosphotransacetylase (*pta*) promoter, rho-independent terminator, ColE1 ori, and repB ori. The antibody resistance genes provides the selection marker for bacteria strains that carries the plasmids (ampicillin for *E.coli* and erythromycin for *C. ljungdahlii*). The *pta* promoter was previously used to express Halotag in *C. ljungdahlii* and was proven to express high fluorescent intensity[34]. Also, Halotag was designed to attach to the C-terminus of the protein to minimize the effect of attaching a bulky fluorescent protein because the N-terminus of MCP generally pass through the cell membrane[23].

The plasmid vector p100ptaCA-Halo and p100MCP-Halo and was constructed to express the fluorescent fused protein of interest using pta promoter, which was established as a strong promoter in *Clostridium* species of interest in previous studies in the lab[34]. *C. ljungdahlii* genomic DNA was extracted using the DNeasy Blood and Tissue Kit (Qiagen). The proteins of interest were cloned from the genomic DNA using Phusion High Fidelity DNA polymerase. Table 1 lists the primers used in plasmid construction. All primers above were designed with sticky ends. MCP was cloned with primer P1 and P2, and CA was cloned with primer P3 and P4. The genes of interest were gel purified using the Nucleospin Gel and PCR Clean-up kit (Macherey-Nagel). An Integrated DNA Technologies gblock containing the promoter, *Clostridium* codon optimized Halotag sequence, and terminator In the gblock design a BamHI restriction digest site is inserted in between pta promoter and the fluorescent protein sequence. The p100MCS vector[44] were digested by Fast Digest SacI and

EcoRI to create an opening to insert the gblock using NEB Hifi DNA assembly kit. Then, the BamHI site on the vector is digested leaving a complementary site to the sticky ends of the cloned protein of interest using Gibson Assembly. The plasmids were screened with colony PCR using Phire Hot Start II DNA polymerase with primer P5 and P6 that binds to the ErmR and terminator region of the plasmid and the colony with the correct band size were selected. Then the correct plasmid is extracted using QIAprep Spin Miniprep Kit (Qiagen). The plasmid is sent to Genewiz (South Plainfield, NJ) for Sanger sequencing to ensure the correct construct was obtained. The plasmid construct can be seen in Figure 3.2.1.

Table 1 Primers used in plasmid construction

Primer Name	Forward or reverse	Sequence (5'→3')
P1	F	aggattagtcTTGAACAGTGATTTTGCTG
P2	R	ctccacctccAAGTTTTTCCACTTCGAAATTC
P3	F	aggattagtcATGTTTAATTTTAAAAGTATTAAAACTAAGTTAATAC
P4	R	ctccacctccTTCTACTTTAAATTTATTTACAACATTTATTAAG
P5	F	TTCCTGAGCCGATTTCAAAG
P6	R	GAGTCAGTGAGCGAGGAAGC

A

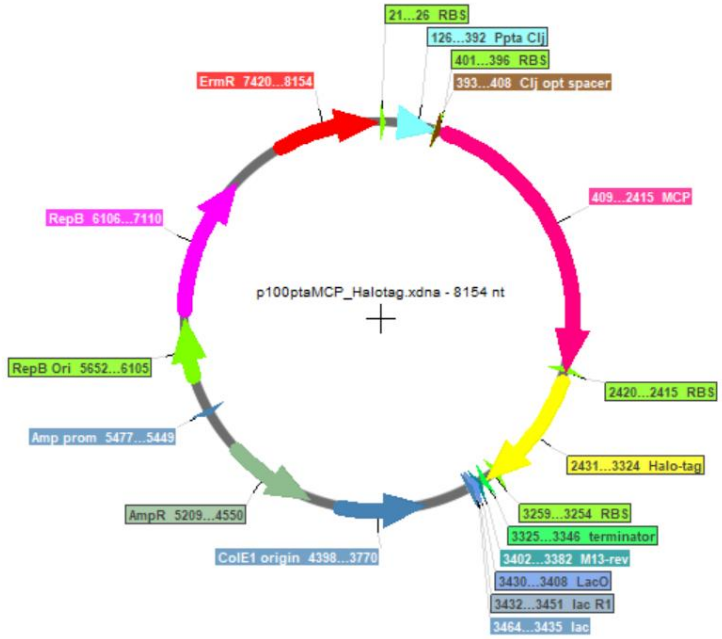

B

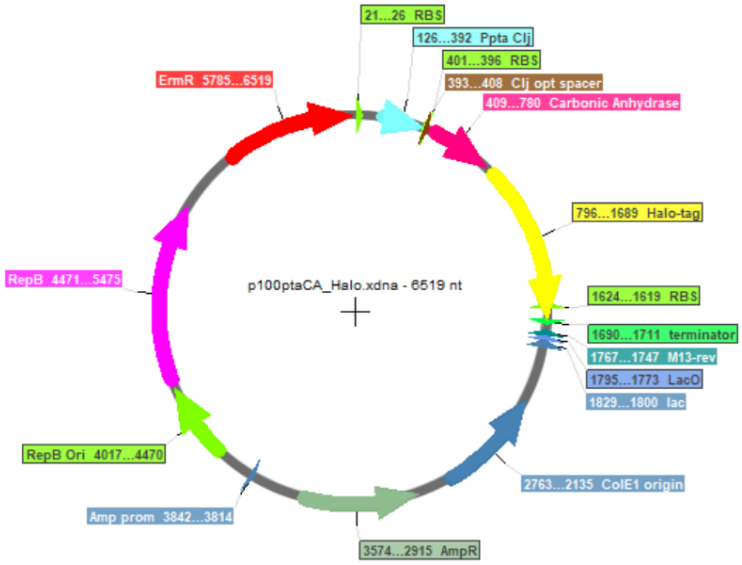

Figure.3.2.1 Plasmid graphic map for fluorescent fused protein generated in Serial cloner **A**. p100ptaMCP-Halotag **B**. p100ptaCA-Halotag.

3.2.4 Vector transformation

The vector plasmid was transformed in 5-α E. coli to propagate and 10-β E. coli for the correct methylation pattern to be transformed into *C. ljungdahlii.* The *C. ljungdahlii* transformation protocol used was previously established[45]. *C. ljungdahlii* was grown in 90mL of ATCC 1754 media to OD_{600} of 0.2-0.3, the cells were collected via anaerobic centrifugation, then washed twice by SMP buffer, and cells are resuspended in 150 µL of antifreezing buffer. For each transformation, 25 µL of *C. ljungdahlii* cells were mixed with 1µg of plasmid DNA and were transferred to 1mm cuvette. Electroporation was carried out at voltage 625V, resistance 600Ω and capacity 25 µF. Then cells were transferred to 5mL of ATCC 1754 media to outgrow for 24 hours. The cells were harvested by centrifugation and resuspended in 1mL of ATCC 1754. The cells were plated with RCM molten agar with 100µg/mL Erythromycin. Solidified plates were left in 37ºC anaerobic incubator for 3 to 5 days. *C. ljungdahlii* colonies imbedded in the agar are collected and inoculated into 5mL of Turbo CGM media with 100µg/mL Erythromycin, then passaged into serum bottle containing 20mL of Turbo CGM media with 100µg/mL Erythromycin and apply 20 psi overhead pressure with 887 gas mix.

3.2.5 Fluorescent labeling of cells

Halotag fluorescent proteins expressing cells were labeled with 200nM of fluorescent ligand. The ligand used were Jenalia Fluor 646 ($\lambda_{excitation}$=646nm, $\lambda_{emission}$=664nm) and TMR Direct Halotag ($\lambda_{excitation}$=552nm, $\lambda_{emission}$=578nm) (Promega). Once the cell sample was mixed by vortex, they were incubated at 37 ºC, aerobically for *E.coli* and anaerobically for *C. ljungdahlii*, for 15-30 minutes. No washing step is required for the two ligands described above.

3.2.6 Dragonfly Spinning Disk and Super Resolution Microscopy

To visualize the fluorescence of the bacteria strains. 200 µL of Halotag labeled cells were seeded onto poly-L-lysine coated coverslip (ThermoFisher) and were incubated anaerobically for 30 to 60 minutes to immobilize the cells. After incubation, cells were rinsed three times with PBS to remove free-floating cells. Then the coverslip was mounted onto the slide and sealed. Dragonfly Spinning Disk and Super Resolution Microscopy was used to image the cells with 63X oil objective. A 633nm red laser was used to visualize red fluorescent from Jenalia 646 labelled cells and 560nm green laser was used to visualize orange fluorescent from TMR Direct Halotag labeled cells. An open sourced imagine processing software FIJI ImageJ was used to analyze the image.

3.2.7 Flow cytometry

Fluorescent cells were screened with Beckman Coulter CytoFLEX S flow cytometer. A red solid-state laser (633 nm excitation) and 660/20 nm filter was used to measure the red fluorescent of Jenalia Fluor 646 ligand bound to the Halotag. FITC-A fluorescent channel was used for 20000 events, and the percentage of the fluorescent event was taken. To prepare the sample 2-5 µL of the cells sample were added to 500uL of the PBS solution. The unlabeled sample lacks the fluorescent ligand

3.3 Results and discussion

3.3.1 Prescence of fluorescence in shuttle strain of *E. coli* under microscopy

The expression of FAST fluorescent fused protein (ZapA-FAST) in *E. coli* shuttle vector has been previously established[35]. Although theoretically, Halotag fluorescent fused protein would be functional and localized in the bacteria cells, no

previous established system was found. Thus, as a preliminary screening, the strain of 10β *E. coli* containing fluorescent fused protein was first observed under the microscope to ensure the functionality of Halotag when attached to a protein.

Images in Figure 3.3.1 are taken with Dragonfly Spinning Disk and Super Resolution Microscopy. Figure.3.3.1.A and Figure.3.3.1 C are unlabeled 10β *E.coli* CA-Halotag and MCP-Halotag respectively. And Figure.3.3.1.B are TMR Direct Halotag labeled 10β *E.coli* MCP-Halotag. Figure.3.3.1.D is Jenalia 646 labeled 10β *E.coli* CA-Halotag. The Halotag protein was present everywhere in the cell cytoplasm, meaning no localization of these proteins is present in *E. coli*. Even though it was reported that *E.coli* also uses MCP as one of its chemotactic receptors[43]. These fluorescent fusion proteins are not localized, which shows that this MCP derived from a *Clostridium* genome is incompatible with *E. coli*. However, this shows that when attached to a protein Halotag can still be fluorescent and could be used as a fluorescent reporter for any future protein localization investigation.

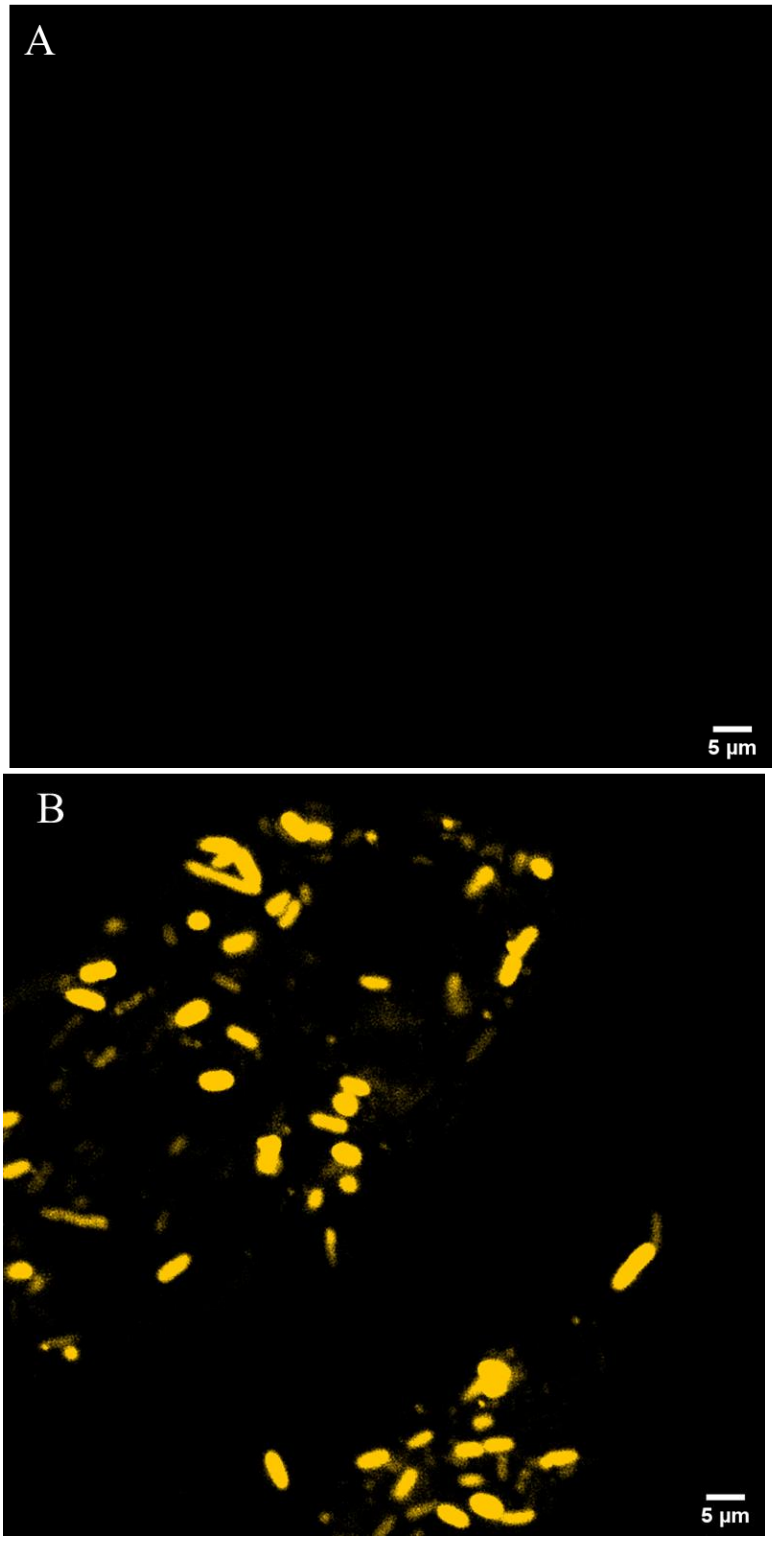
A
5 µm
B
5 µm

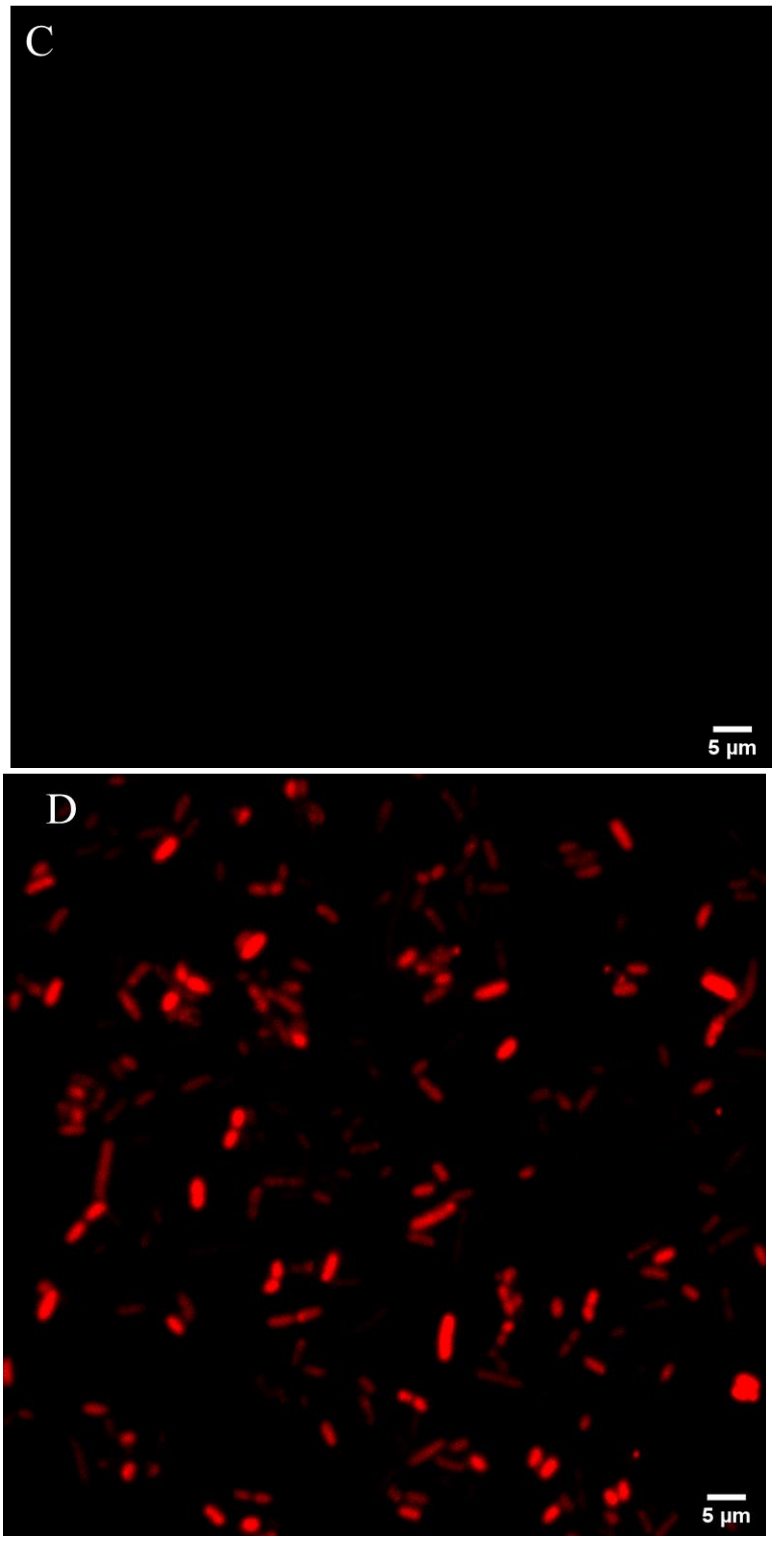
C
5 µm
D
5 µm

Figure.3.3.1 Microscopy image of 10β *E. coli* **A**. unlabeled 10β *E. coli* CA-Halotag **B**. TMR Direct Halotag labeled 10β *E. coli* CA-Halotag. **C**. unlabeled 10β *E. coli* MCP-Halotag. **D.** Jenalia 646 labeled 10β *E. coli* MCP-Halotag

3.3.1 MCP-Halotag exhibits cell membrane localization in *C. ljungdahlii*

The previous section of *E.coli* microscopy has demonstrated the fluorescence of MCP-Halotag and CA-Halotag, although no localization was observed, it is very likely that *E. coli* cells failed to recognize the *C. ljungdahlii* proteins, meaning it is possible that *E.coli* failed to fold and utilize the MCP-Halotag protein.

The fluorescent intensity of the fluorescent fused proteins were first tested on the flow cytometer, the results are shown in Figure 3.3.2. Compared to the unlabeled cells, the labeled MCP and CA cells expressed a 79% and 91% fluorescent population (Figure 3.3.2.B and Figure 3.3.2.D). In Figure.3.3.2. D, the flow cytometry result for MCP-Halotag showed different peaks, this is likely due to the difference in the MCP-Halotag expression in different cells. These results demonstrate a clear distinction in fluorescence between cells that express ligand labeled fluorescent fused proteins and the cells that do not. Also, the high fluorescence expression in both cell populations showed the fluorescent fused proteins were highly expressed.

C. ljungdahlii slides were prepared anaerobically and were imagined using the Dragonfly Spinning Disk and Super Resolution microscope. Protein localization with *C. ljungdahlii* can be seen in Figure 3.3.3. More images are shown in the Supplementary document. To visualize the fluorescent localization better, the Jenalia 646 *C. ljungdahlii* CA-Halotag and Jenalia 646 *C. ljungdahlii* MCP-Halotag are shown under different red fluorescent intensities (Figures 3.3.3.A and B). CA-Halotag

in *C. ljungdahlii* exhibits no localization as the fluorescent signal can be observed all over the cell cytoplasm. The difference in fluorescent intensity observed is due to the fact that the cells do not adhere to the slide on a uniform plane, and therefore some parts of the cells were further or closer to the plane of the image taken. Localization was observed in *C. ljungdahlii* MCP-Halotag (Figure 3.3.3.A). MCP localizes on the cell membrane in *C. ljungdahlii*. The cell cytoplasm clearly lacks fluorescent signal. This shows that the protein coded by the CLJU_c10160 gene is likely a membrane bound MCP. This also demonstrates that Halotag can be used to create functional fluorescent fusion proteins in *C. ljungdahlii*, as the proteins localization behavior seems not to be affected by the attached Halotag on its C-terminus.

A

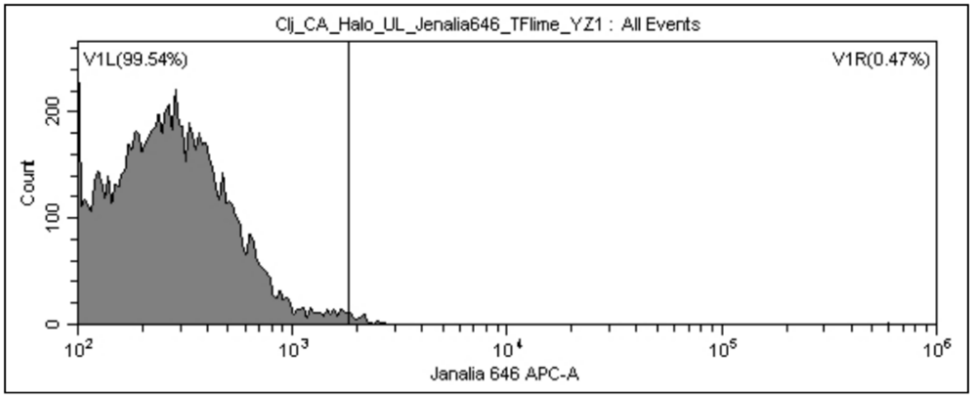

B

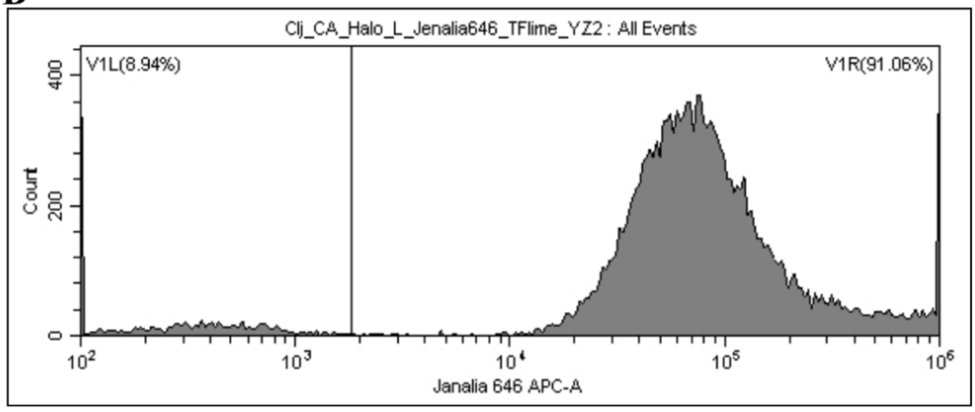

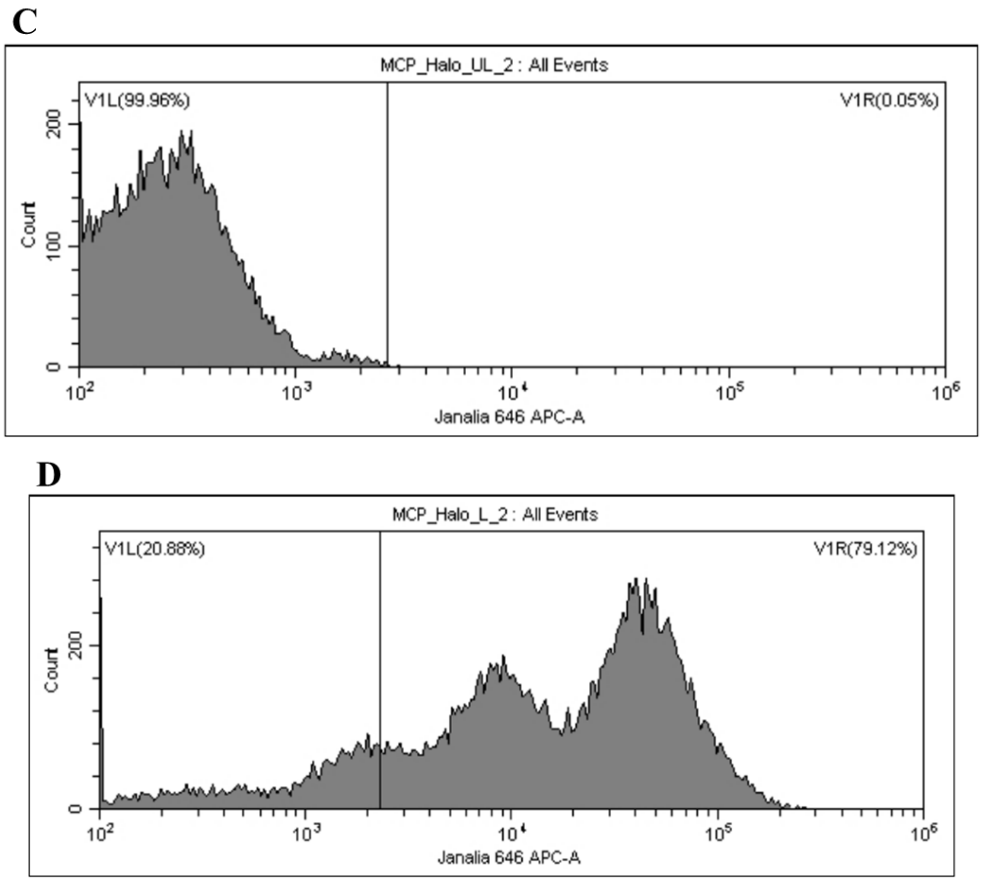

Figure.3.3.2. Flow cytometry fluorescent intensity comparison between unlabled and Janelia 646 labeled cells **A**. Unlabled CA-Halotag. **B**. Labled CA-Halotag. **C**. Unlabled MCP-Halotag. **D**. Labled MCP-Halotag.

A

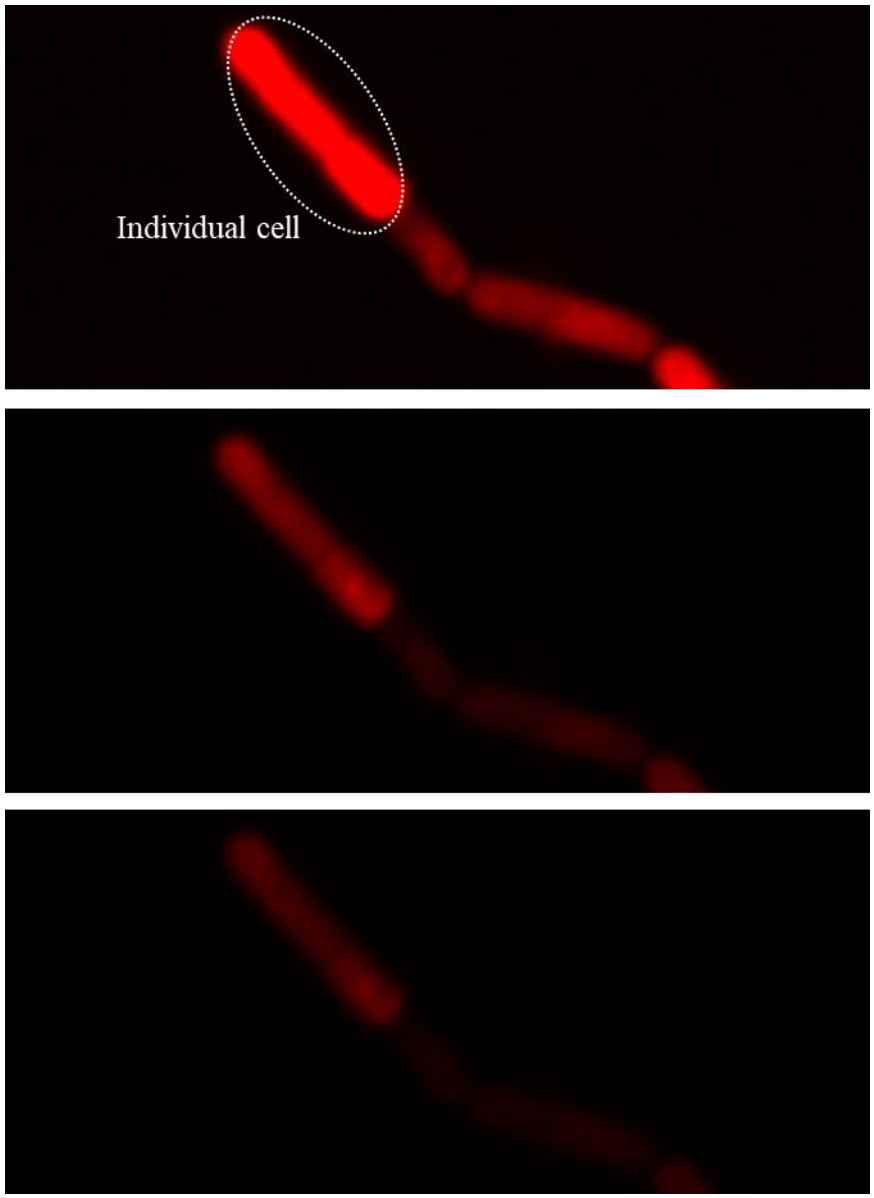

Figure.3.3.3. Microscopy image of *C. ljungdahlii* with adjusted red fluorescent intensity level by fixing minimal brightness display value to 0 and varying max brightness display value to 1000,3000 and 5000 (brightest to dimmest) **A**. Janelia 646 labeled MCP-Halotag **B**. Janelia 646 labeled CA-Halotag

3.3.2 Discussion

As shown in the sections above, CA-Halotag and MCP Halotag exhibit strong fluorescence in both *E.coli* and *C. ljungdahlii*. MCP-Halotag exhibits localization on the cell membrane and a visually even distribution on cell membrane. Both polar and lateral localization patterns of MCPs were observed. Due to a lack of understanding of MCP in *C. ljungdahlii*, there are no previous studies to compare the localization pattern. However, this shows the predicted MCP (CLJU_c10160) encoded in *C. ljungdahlii* genome is a transmembrane protein, and *C. ljungdahlii* could recognize and incorporate the MCP into its cell membrane, and likely the cell utilizes MCP as a chemoreceptor. Although no previous studies have shown the localization pattern of MCP in *Clostridium* species, a similar polar and lateral localization pattern was reported for the WspA receptor protein in *Pseudomonas aeruginosa*, a protein that is bioinformatically indistinguishable from MCP[27]. In the reported study, 62% of the WspA protein localized on the lateral sides of the cell, and the remaining localized on polar ends[27].

Aside from MCP localization, CA did not exhibit localization patterns in either *E. coli* or *C. ljungdahlii*. Since *C. ljungdahlii* is a Gram positive bacterium, a β- or γ-CA is the expected type of CA, and such Cas have a cytoplasmic localization. Although it is possible that the CA could show localized expression, because the culture was incubated in a shaker, the constant mixing leads to a uniform distribution of nutrients or CO_2 gas in the liquid culture. Therefore, there is no CO_2 concentration gradient in the culture to enable a possible CA polar localization.

With the success of a strong Halotag based fluorescent fused protein exhibiting MCP localization in *C. ljungdahlii*, more protein localization studies could be conducted. This study has expanded the toolkit for protein functionality studies in

Clostridium species. The localization of MCP in *C. ljungdahlii* have aided our understanding of sensory mechanism in *C. ljungdahlii*. Future work could examine protein localization in *C. acetobutylicum* and *C. ljungdahlii* co-cultures.

Chapter 4

Conclusion and future works

4.1.1 Conclusions

In this thesis, optimization of hexanoate production in *Clostridium* co-culture was investigated. In the original design, *C. kluyveri* and *C. acetobutylicum* co-culture was proposed. However, the two species operate under different optimal pH. *C. acetobutylicum* prefers more acidic condition and *C. kluyveri* prefer neutral pH. *C. kluyveri* monocultures were initially examined under different pH conditions. *C. kluyveri* exhibits hexanoate production at pH above 6.0 (Figure 2.3.1). *C. acetobutylicum* has been reported to express autolytic behavior when pH is above 6[4]. This result enhanced the initial speculations about incompatible pH of the two species. Therefore, the performance of both organisms would be limited. To resolve the issue, co-culture with ethanologenic *C. saccharolyticum* was proposed. *C. saccharolyticum* has been reported to perform optimally under neutral pH and consume sugars to produce ethanol and acetate[10].

To first assess hexanoate production of *C. kluvyeri*, an optimized *C. kluyveri* monoculture with controlled pH level, and ethanol and acetate concentrations was tested (Figure 2.3.2). Under the tested conditions, *C. kluyveri* produced an unprecedented 173mM of Hexanoate in 45 hours (Figure 2.3.2.C). The tested *C. saccharolyticum* and *C.kluvyeri* co-culture exhibited strong hexanoate production, with 124 mM of hexanoate produced in 70 hours (54 hours after *C. kluyveri* inoculation) (Figure 2.3.3). Hexanoate production was apparently limited by ethanol production by *C. saccharolyticum*. The initially accumulated 148 mM of ethanol was quickly depleted in the culture (Figure 2.3.3.C). Although the co-culture hexanoate

productivity could not match the *C. kluyveri* monoculture, the co-culture result still exhibited promising hexanoate production and possible space for improvements.

Investigation of the fluorescent fused proteins showed that the Halotag based fluorescent system could work in protein localization studies in *C. ljungdahlii.* The proteins of interest in this study were CA and MCP, two proteins that were hypothesized to be involved in CO_2 sensing and metabolism by *C. ljungdahlii*. Therefore, observing their localization could help elucidate their functionality. First, the fluorescent intensity of the Halotag fused proteins were tested with flow cytometry (Figure 3.3.2). The results showed significantly different fluorescent intensity between cells with Janelia 646 bound Halotag fused protein and cells without.

In Figure 3.3.3, the microscopic image of *C. ljungdahlii* with CA-Halotag and with MCP-Halotag is shown. Both fluorescent fused proteins showed strong fluorescence under microscopic observation. In MCP-Halotag cells (Figure 3.3.3. A), membrane localization of the protein was observed, although there was no obvious lateral or polar localization pattern observed as commonly reported in other MCP or MCP-like proteins[23]. This result showed that fusing the protein with Halotag would not affect the localization pattern of the protein. In CA-Halotag cells (Figure 3.3.3. B), CA did not appear to localize in the cells, but was evenly distributed throughout the cytoplasm. This result agrees with the cytoplasmic expression of β- and γ-CAs reported in Gram positive bacteria[13]

4.2 Future work

4.2.1 Future work for *Clostridium* co-culture optimization

In the *C. saccharolyticum* and *C. kluyveri* co-culture experiment described above, the drawback of the system is likely to be the insufficient ethanol productivity of *C. saccharolyticum* to supply the need of *C. kluyveri.* One possible improvement to the system could be incorporating *C. ljungdahlii* to recover the CO_2 produced by *C. saccharolyticum* and not used by *C. kluyveri* . This way, *C. ljungdahlii* would also supply additional ethanol and acetate to *C. kluyveri*. *C. ljungdahlii* would also convert the fatty acid produced by *C. kluyveri* into their corresponding alcohols[2]. Also, possible modifications to the current system of co-culture could be further optimized. Currently, the bioreactors operate as a fed-batch reactor, only supplying glucose as the carbon source and base to control the pH. Future improvements could involve supplying additional nutrients such as vitamins and minerals to the cells during the fermentation to prolong the cell proliferation, which could aid in the chemical productivity of the bacteria. Also, development of an *in situ* product separation scheme in the bioreactors could prevent the toxicity of highly concentrated products to the cells. Improved design to the bioreactor operation scheme could also be considered, such as a continuous bioreactor in series. *C. saccharolyticum* can be grown in a separate bioreactor with continuous feed of fresh media and the effluent can enter a secondary reactor for *C. saccharolyticum* and *C. kluyveri* co-culture. Thus, *C. saccharolyticum* could accumulate high ethanol concentration in the first reactor and medium chain fatty acid can be synthesized in the secondary reactor.

4.2.2 Fluorescent protein localization in *C. ljungdahlii*

For future fluorescent fusion protein work, a *C. acetobutylicum* and *C. ljungdahlii* co-culture utilizing the MCP-Halotag and CA-Halotag *C. ljungdahlii* strains could be tested. As *C. acetobutylicum* produces CO_2 as waste gas, it might trigger localization of the MCP and CA proteins if they are involved in CO_2 sensing. Observing the protein localization patterns within the co-culture under the microscope might help to test if the proteins are involved in the cell fusion and direct material exchange between *C. ljungdahlii* and *C. acetobutylicum*[1]. Additionally, the fluorescent fused protein plasmid constructed for this study could be utilized to fuse other proteins of interest in future studies.

4.2.3 Final remark

In this undergraduate thesis, the co-culture optimization yielded promising results in the hexanoate production which further supported the co-culture could make *Clostridium* fermentation could be industrially and economically significant. The fluorescent protein study showed the localization patterns and the feasibility of observing MCP and CA with Halotag fusion. This work expanded the toolkit for future protein localization studies.

For future studies derived from this project, possible further enhancement in the *C. saccharolyticum* ethanol productivity in the co-culture and development of *C. saccharolyticum*, *C. kluyveri*, and *C. ljungdahlii* co-culture may bring more insights for exploring the industrial potential of *Clostridium* fermentation processes. Examination of *C. acetobutylicum* and *C. ljungdahlii* cells in co-culture using the strains developed in this project may help elucidate the mechanism of cell to cell

direct material exchange, which will enable the development of more efficient co-culture systems.

The work done in this thesis not only serves as excellent research and learning experience for the students but also would aid future co-culture research about cell interaction or addition of other species of *Clostridium* to further improve the production of valuable metabolites.

Appendix A Bacterial strains, plasmid used in this study

Table A.1 Strains and plasmids used in the fluorescent and co-culture study

Strain	Relevant Characteristics	Source
E.Coli		
NEB 5-alpha	*fhuA2 Δ(argF-lacZ)U169 phoA glnV44 Φ80 Δ(lacZ)M15 gyrA96 recA1 relA1 endA1 thi-1 hsdR17*	**NEB**
NEB 10-beta	*Δ(ara-leu) 7697 araD139 fhuA ΔlacX74 galK16 galE15 e14ϕ80*d*lacZΔM15 recA1 relA1 endA1 nupG rpsL*(Str^R)*rph spoT1Δ(mrr-hsdRMS-mcrBC)*	**NEB**
C.ljundahlii		
ATCC 55383	Wild-type strain	**ATCC**
C.kluyveri		
ATCC 8527	Wild-type strain	**ATCC**
C.saccharolyticum		
ATCC35040	Wild-type strain	**ATCC**
Plasmids		
P100_MCS	*thl* promoter, *Amp$_r$ ErmR ColE1Ori repB, MCS*	Fast and Papoutsakis 2018
P100CA-Halo	*pta* promoter, *Amp$_r$ ErmR ColE1Ori repB CA Halotag*	This study
P100Meche-FAST	*pta* promoter, *Amp$_r$ ErmR ColE1Ori repB Meche Halotag*	This study

Appendix B Additional images from fluorescent fused protein study

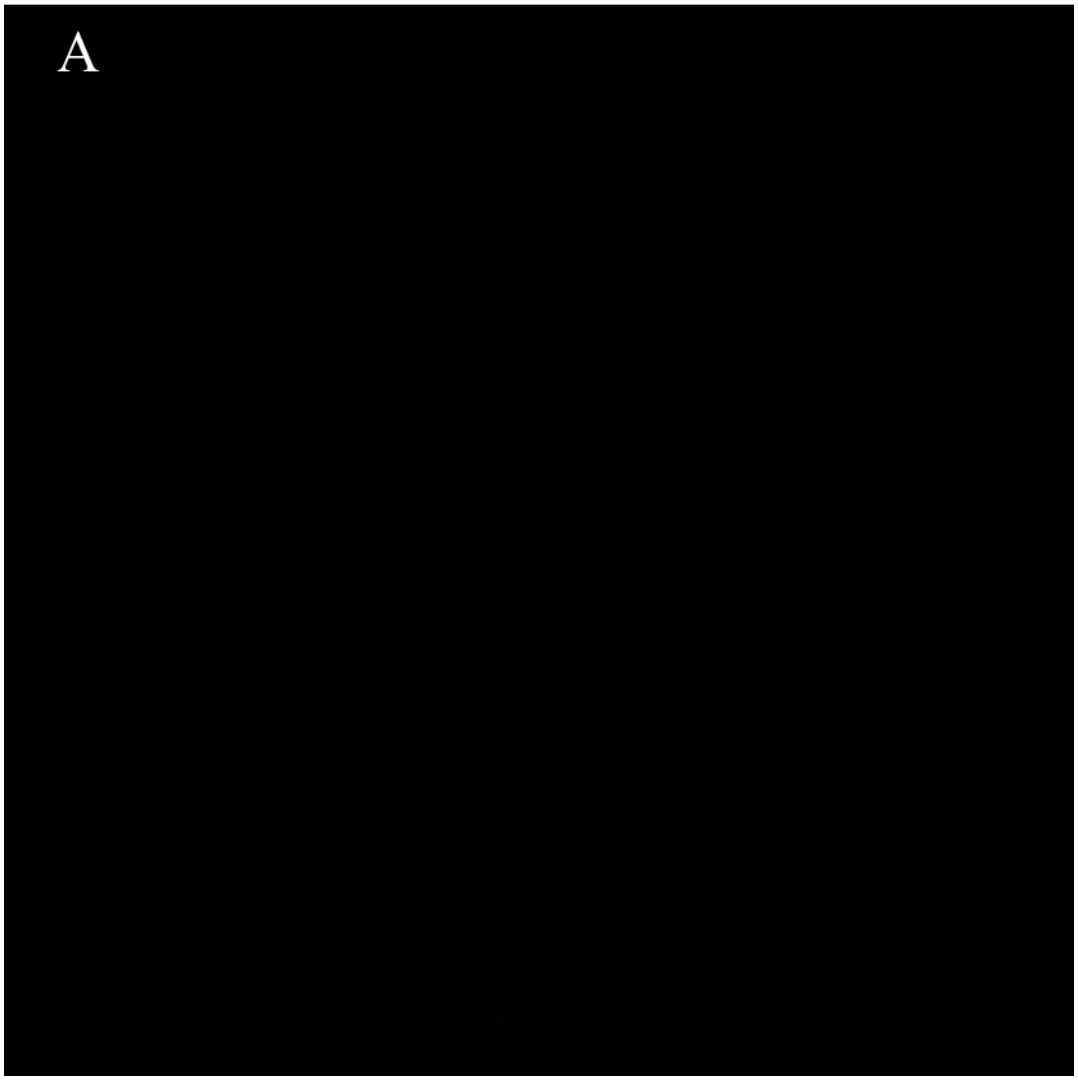

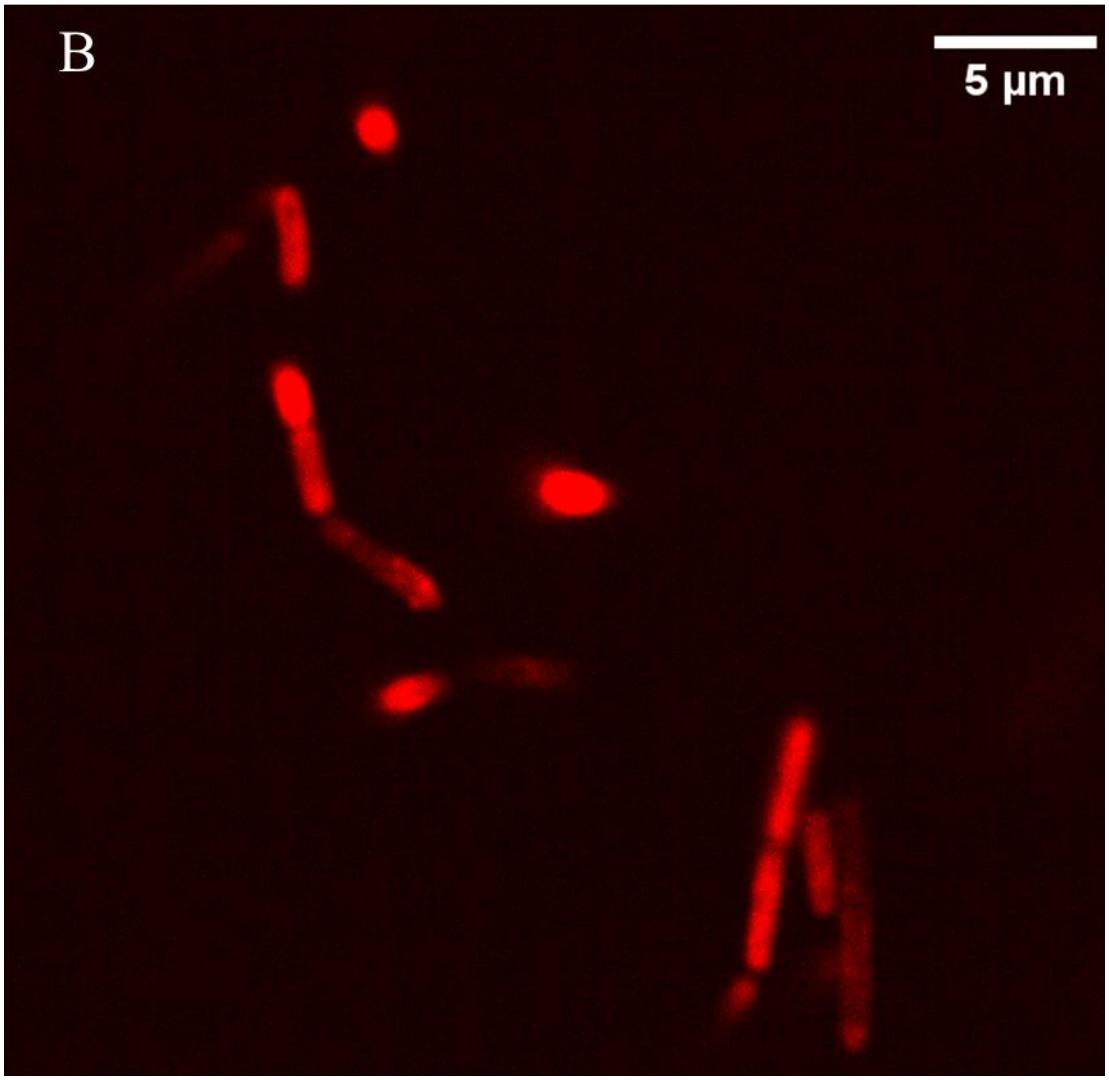
B
5 µm

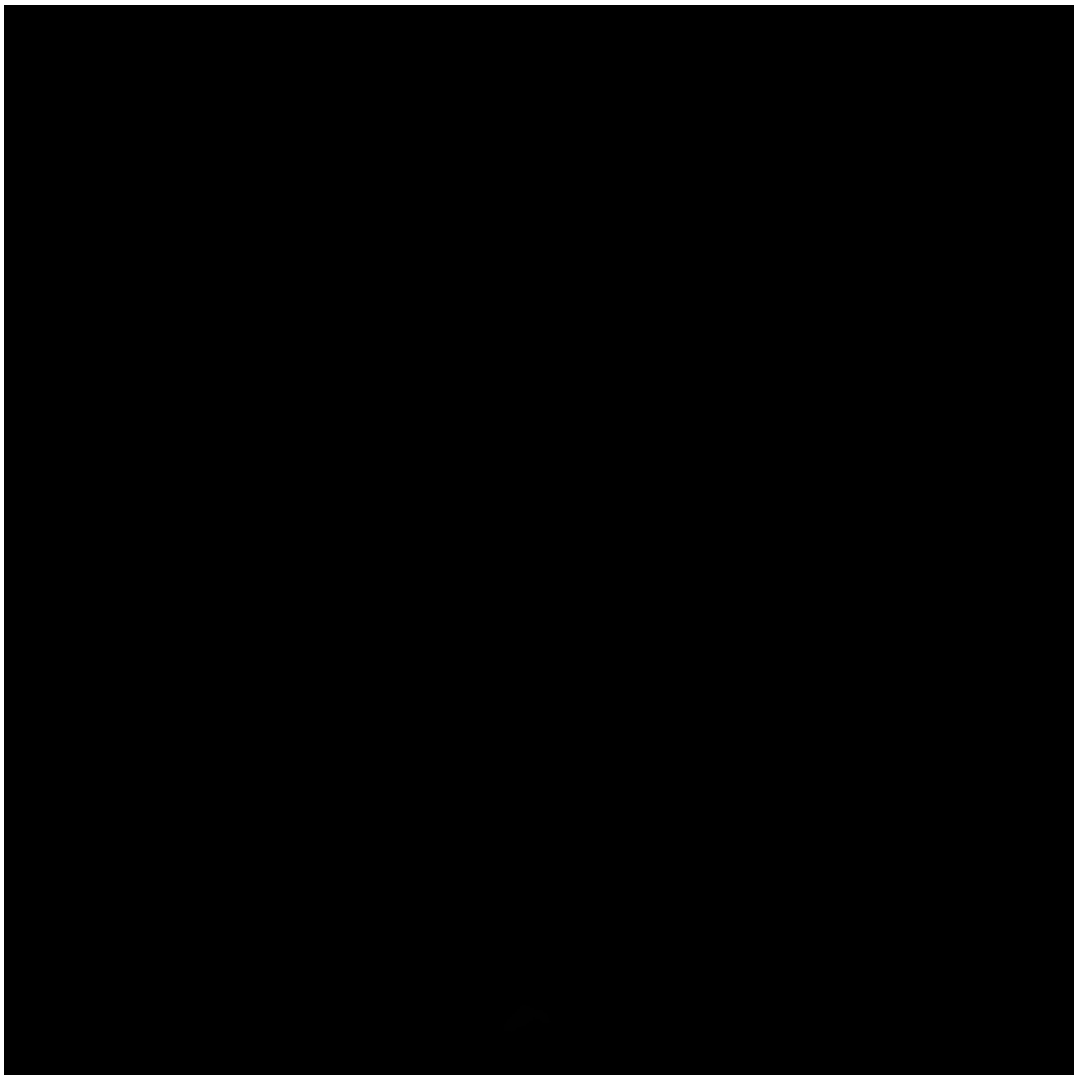

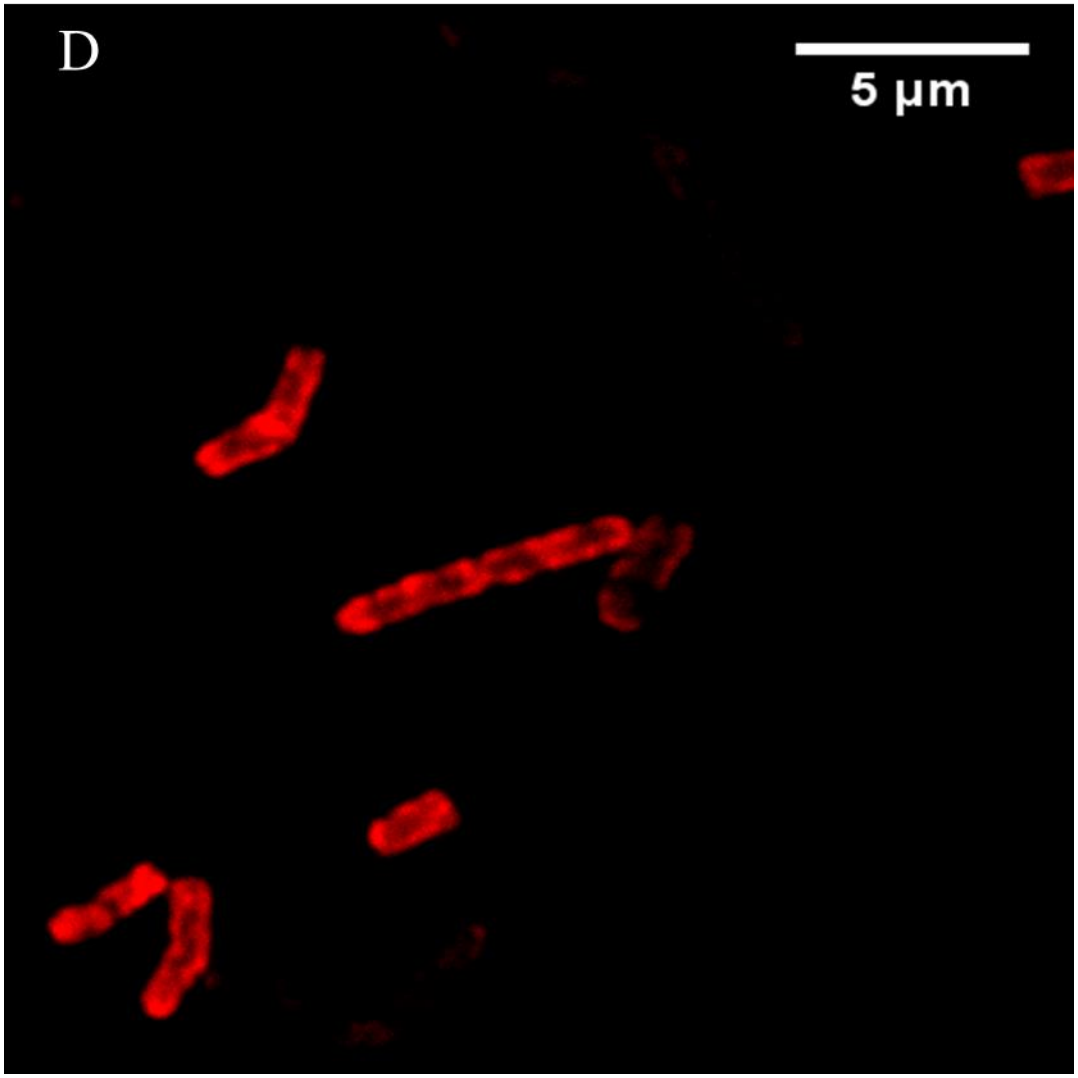

Figure .B.1 Additional microscopic image of C. ljungdahlii **A**. unlabeled C. ljungdahlii CA-Halotag **B**. TMR Direct Halotag labeled **C**. ljungdahlii CA-Halotag. C. unlabeled C. ljungdahlii MCP-Halotag. **D**. Jenalia 646 labeled C. ljungdahlii MCP-Halotag

A

B

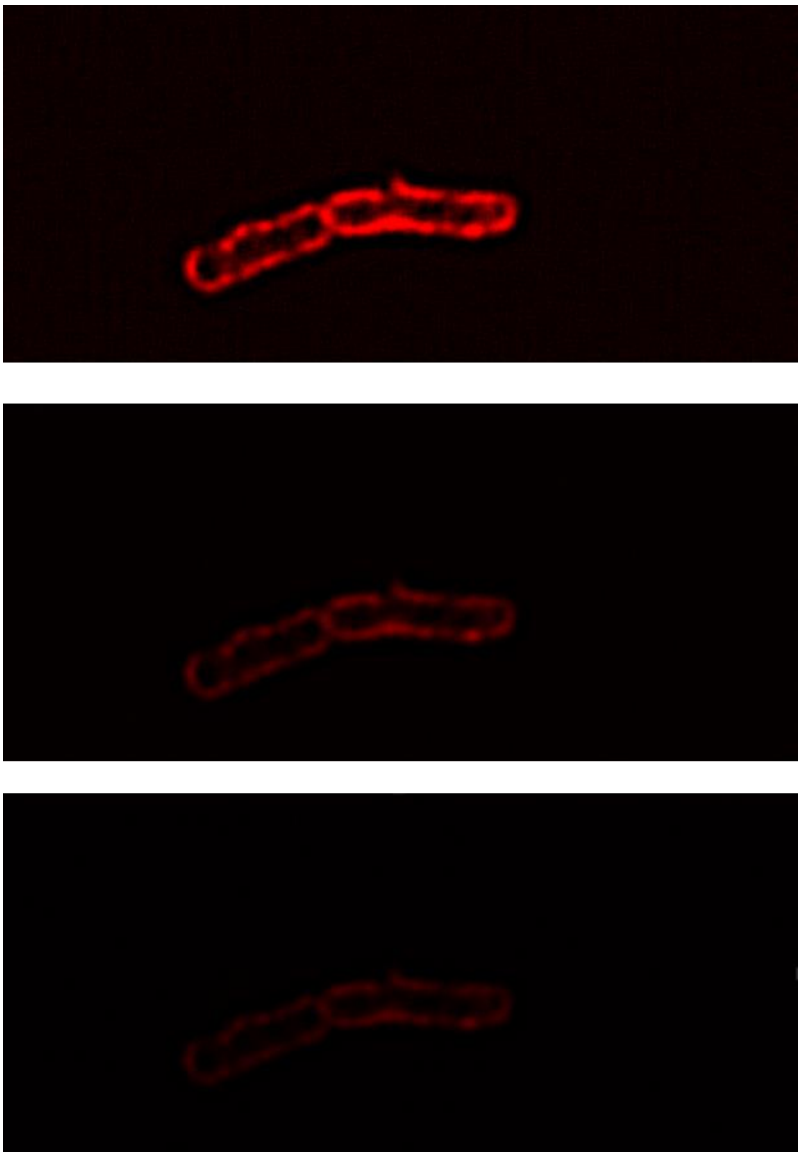

C

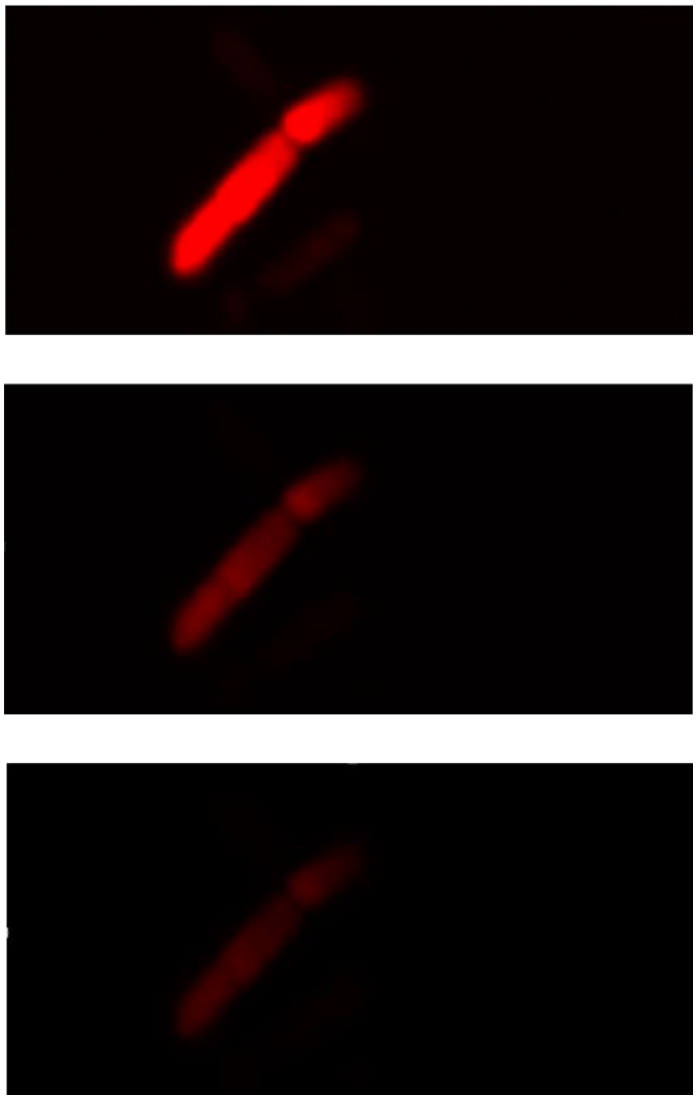

Figure.B.2 Additional microscopic image of C. ljungdahlii with adjusted red fluorescent intensity level by fixing minimal brightness display value to 0 and varying max brightness display value to 1000,3000 and 5000 (brightest to dimmest) **A**. Extra-1 Janelia 646 labeled MCP-Halotag **B**. Extra-2 Janelia 646 labeled MCP-Halotag **C**. Janelia 646 labeled CA-Halotag

References

(1) Charubin, K.; Papoutsakis, E. T. Direct cell-to-cell exchange of matter in a synthetic Clostridium syntrophy enables CO2 fixation, superior metabolite yields, and an expanded metabolic space. *Metabolic Engineering* **2019**, *52*, 9-19. DOI: https://doi.org/10.1016/j.ymben.2018.10.006.

(2) Tracy, B. P.; Jones, S. W.; Fast, A. G.; Indurthi, D. C.; Papoutsakis, E. T. Clostridia: the importance of their exceptional substrate and metabolite diversity for biofuel and biorefinery applications. *Curr Opin Biotechnol* **2012**, *23* (3), 364-381. DOI: 10.1016/j.copbio.2011.10.008 From NLM.

(3) Gyulev, I. S.; Willson, B. J.; Hennessy, R. C.; Krabben, P.; Jenkinson, E. R.; Thomas, G. H. Part by Part: Synthetic Biology Parts Used in Solventogenic Clostridia. *ACS Synth Biol* **2018**, *7* (2), 311-327. DOI: 10.1021/acssynbio.7b00327 From NLM.

(4) Roos, J. W.; McLaughlin, J. K.; Papoutsakis, E. T. The effect of pH on nitrogen supply, cell lysis, and solvent production in fermentations of Clostridium acetobutylicum. *Biotechnol Bioeng* **1985**, *27* (5), 681-694. DOI: 10.1002/bit.260270518 From NLM.

(5) Grupe, H.; Gottschalk, G. Physiological Events in Clostridium acetobutylicum during the Shift from Acidogenesis to Solventogenesis in Continuous Culture and Presentation of a Model for Shift Induction. *Applied and Environmental Microbiology* **1992**, *58* (12), 3896-3902. DOI: 10.1128/aem.58.12.3896-3902.1992 (acccessed 2022/04/25).

(6) Tanner, R. S.; Miller, L. M.; Yang, D. Clostridium ljungdahlii sp. nov., an acetogenic species in clostridial rRNA homology group I. *Int J Syst Bacteriol* **1993**, *43* (2), 232-236. DOI: 10.1099/00207713-43-2-232 From NLM.

(7) Charubin, K.; Bennett, R. K.; Fast, A. G.; Papoutsakis, E. T. Engineering Clostridium organisms as microbial cell-factories: challenges & opportunities. *Metabolic Engineering* **2018**, *50*, 173-191. DOI: https://doi.org/10.1016/j.ymben.2018.07.012.

(8) Seedorf, H.; Fricke, W. F.; Veith, B.; Brüggemann, H.; Liesegang, H.; Strittmatter, A.; Miethke, M.; Buckel, W.; Hinderberger, J.; Li, F.; et al. The genome of Clostridium kluyveri, a strict anaerobe with unique metabolic features. *Proceedings of the National Academy of Sciences* **2008**, *105* (6), 2128-2133. DOI: 10.1073/pnas.0711093105 (acccessed 2022/04/25).

(9) Gildemyn, S.; Molitor, B.; Usack, J. G.; Nguyen, M.; Rabaey, K.; Angenent, L. T. Upgrading syngas fermentation effluent using Clostridium kluyveri in a continuous fermentation. *Biotechnology for Biofuels* **2017**, *10* (1), 83. DOI: 10.1186/s13068-017-0764-6.

(10) MURRAY, W. D.; KHAN, A. W.; van den BERG, L. Clostridium saccharolyticum sp. nov., a Saccharolytic Species from Sewage Sludge†. *International Journal of Systematic and Evolutionary Microbiology* **1982**, *32* (1), 132-135. DOI: https://doi.org/10.1099/00207713-32-1-132.

(11) Haas, K. N.; Blanchard, J. L. Reclassification of the Clostridium clostridioforme and Clostridium sphenoides clades as Enterocloster gen. nov. and Lacrimispora gen. nov., including reclassification of 15 taxa. *Int J Syst Evol Microbiol* **2020**, *70* (1), 23-34. DOI: 10.1099/ijsem.0.003698 From NLM.

(12) Morris, B. E. L.; Henneberger, R.; Huber, H.; Moissl-Eichinger, C. Microbial syntrophy: interaction for the common good. *FEMS Microbiology Reviews* **2013**, *37* (3), 384-406. DOI: 10.1111/1574-6976.12019 (acccessed 4/25/2022).

(13) Supuran, C. T.; Capasso, C. An Overview of the Bacterial Carbonic Anhydrases. *Metabolites* **2017**, *7* (4). DOI: 10.3390/metabo7040056 From NLM.

(14) Kusian, B.; Sültemeyer, D.; Bowien, B. Carbonic anhydrase is essential for growth of Ralstonia eutropha at ambient CO(2) concentrations. *J Bacteriol* **2002**, *184* (18), 5018-5026. DOI: 10.1128/jb.184.18.5018-5026.2002 From NLM.

(15) Capasso, C.; Supuran, C. T. An overview of the alpha-, beta- and gamma-carbonic anhydrases from Bacteria: can bacterial carbonic anhydrases shed new light on evolution of bacteria? *Journal of Enzyme Inhibition and Medicinal Chemistry* **2015**, *30* (2), 325-332. DOI: 10.3109/14756366.2014.910202.

(16) Supuran, C. T.; Capasso, C. New light on bacterial carbonic anhydrases phylogeny based on the analysis of signal peptide sequences. *J Enzyme Inhib Med Chem* **2016**, *31* (6), 1254-1260. DOI: 10.1080/14756366.2016.1201479 From NLM.

(17) Kumar, R. S. S.; Hendrick, W.; Correll Jared, B.; Patterson Andrew, D.; Melville Stephen, B.; Ferry James, G. Biochemistry and Physiology of the β Class Carbonic Anhydrase (Cpb) from Clostridium perfringens Strain 13. *Journal of Bacteriology* **2013**, *195* (10), 2262-2269. DOI: 10.1128/JB.02288-12 (acccessed 2022/04/23).

(18) Pander, B.; Harris, G.; Scott, D. J.; Winzer, K.; Köpke, M.; Simpson, S. D.; Minton, N. P.; Henstra, A. M. The carbonic anhydrase of Clostridium autoethanogenum represents a new subclass of β-carbonic anhydrases. *Applied Microbiology and Biotechnology* **2019**, *103* (17), 7275-7286. DOI: 10.1007/s00253-019-10015-w.

(19) Hickman, J. W.; Tifrea, D. F.; Harwood, C. S. A chemosensory system that regulates biofilm formation through modulation of cyclic diguanylate levels. *Proc Natl Acad Sci U S A* **2005**, *102* (40), 14422-14427. DOI: 10.1073/pnas.0507170102 From NLM.

(20) Berleman, J. E.; Bauer, C. E. Involvement of a Che-like signal transduction cascade in regulating cyst cell development in Rhodospirillum centenum. *Molecular Microbiology* **2005**, *56* (6), 1457-1466, https://doi.org/10.1111/j.1365-

2958.2005.04646.x. DOI: https://doi.org/10.1111/j.1365-2958.2005.04646.x (acccessed 2022/04/15).

(21) Luu, R. A.; Kootstra, J. D.; Nesteryuk, V.; Brunton, C. N.; Parales, J. V.; Ditty, J. L.; Parales, R. E. Integration of chemotaxis, transport and catabolism in Pseudomonas putida and identification of the aromatic acid chemoreceptor PcaY. *Molecular Microbiology* **2015**, *96* (1), 134-147, https://doi.org/10.1111/mmi.12929. DOI: https://doi.org/10.1111/mmi.12929 (acccessed 2022/04/15).

(22) Zhulin, I. B. The superfamily of chemotaxis transducers: from physiology to genomics and back. *Adv Microb Physiol* **2001**, *45*, 157-198. DOI: 10.1016/s0065-2911(01)45004-1 From NLM.

(23) Salah Ud-Din, A. I. M.; Roujeinikova, A. Methyl-accepting chemotaxis proteins: a core sensing element in prokaryotes and archaea. *Cellular and Molecular Life Sciences* **2017**, *74* (18), 3293-3303. DOI: 10.1007/s00018-017-2514-0.

(24) Liu, Y. C.; Machuca, M. A.; Beckham, S. A.; Gunzburg, M. J.; Roujeinikova, A. Structural basis for amino-acid recognition and transmembrane signalling by tandem Per-Arnt-Sim (tandem PAS) chemoreceptor sensory domains. *Acta Crystallogr D Biol Crystallogr* **2015**, *71* (Pt 10), 2127-2136. DOI: 10.1107/s139900471501384x From NLM.

(25) Machuca, M. A.; Liu, Y. C.; Beckham, S. A.; Gunzburg, M. J.; Roujeinikova, A. The crystal structure of the tandem-PAS sensing domain of Campylobacter jejuni chemoreceptor Tlp1 suggests indirect mechanism of ligand recognition. *Journal of Structural Biology* **2016**, *194* (2), 205-213. DOI: https://doi.org/10.1016/j.jsb.2016.02.019.

(26) Lacal, J.; García-Fontana, C.; Muñoz-Martínez, F.; Ramos, J. L.; Krell, T. Sensing of environmental signals: classification of chemoreceptors according to the size of their ligand binding regions. *Environ Microbiol* **2010**, *12* (11), 2873-2884. DOI: 10.1111/j.1462-2920.2010.02325.x From NLM.

(27) O'Connor, J. R.; Kuwada, N. J.; Huangyutitham, V.; Wiggins, P. A.; Harwood, C. S. Surface sensing and lateral subcellular localization of WspA, the receptor in a chemosensory-like system leading to c-di-GMP production. *Mol Microbiol* **2012**, *86* (3), 720-729. DOI: 10.1111/mmi.12013 From NLM.

(28) Mauriello, E. M. F.; Jones, C.; Moine, A.; Armitage, J. P. Cellular targeting and segregation of bacterial chemosensory systems. *FEMS Microbiology Reviews* **2018**, *42* (4), 462-476. DOI: 10.1093/femsre/fuy015 (acccessed 4/24/2022).

(29) Charubin, K.; Modla, S.; Caplan Jeffrey, L.; Papoutsakis Eleftherios, T.; Parsek Matthew, R. Interspecies Microbial Fusion and Large-Scale Exchange of Cytoplasmic Proteins and RNA in a Syntrophic Clostridium Coculture. *mBio 11* (5), e02030-02020. DOI: 10.1128/mBio.02030-20 (acccessed 2022/04/25).

(30) Thiem, S.; Sourjik, V. Stochastic assembly of chemoreceptor clusters in Escherichia coli. *Mol Microbiol* **2008**, *68* (5), 1228-1236. DOI: 10.1111/j.1365-2958.2008.06227.x From NLM.

(31) Joseph, R. C.; Kim, N. M.; Sandoval, N. R. Recent Developments of the Synthetic Biology Toolkit for Clostridium. *Frontiers in Microbiology* **2018**, *9*, Mini Review.

(32) Suarez, A.; Güttler, A.; Strätz, M.; Staendner, L. H.; Timmis, K. N.; Guzmán, C. A. Green fluorescent protein-based reporter systems for genetic analysis of bacteria including monocopy applications. *Gene* **1997**, *196* (1), 69-74. DOI: https://doi.org/10.1016/S0378-1119(97)00197-2.

(33) Ransom Eric, M.; Ellermeier Craig, D.; Weiss David, S.; Kivisaar, M. Use of mCherry Red Fluorescent Protein for Studies of Protein Localization and Gene Expression in Clostridium difficile. *Applied and Environmental Microbiology* **2015**, *81* (5), 1652-1660. DOI: 10.1128/AEM.03446-14 (acccessed 2022/04/25).

(34) Charubin, K.; Streett, H.; Papoutsakis Eleftherios, T.; Kelly Robert, M. Development of Strong Anaerobic Fluorescent Reporters for Clostridium acetobutylicum and Clostridium ljungdahlii Using HaloTag and SNAP-tag Proteins. *Applied and Environmental Microbiology 86* (20), e01271-01220. DOI: 10.1128/AEM.01271-20 (acccessed 2022/04/25).

(35) Streett Hannah, E.; Kalis Katie, M.; Papoutsakis Eleftherios, T.; Kivisaar, M. A Strongly Fluorescing Anaerobic Reporter and Protein-Tagging System for Clostridium Organisms Based on the Fluorescence-Activating and Absorption-Shifting Tag Protein (FAST). *Applied and Environmental Microbiology 85* (14), e00622-00619. DOI: 10.1128/AEM.00622-19 (acccessed 2021/12/04).

(36) Sillers, R.; Al-Hinai, M. A.; Papoutsakis, E. T. Aldehyde-alcohol dehydrogenase and/or thiolase overexpression coupled with CoA transferase downregulation lead to higher alcohol titers and selectivity in Clostridium acetobutylicum fermentations. *Biotechnol Bioeng* **2009**, *102* (1), 38-49. DOI: 10.1002/bit.22058 From NLM.

(37) Tummala, S. B.; Welker, N. E.; Papoutsakis, E. T. Development and characterization of a gene expression reporter system for Clostridium acetobutylicum ATCC 824. *Appl Environ Microbiol* **1999**, *65* (9), 3793-3799. DOI: 10.1128/aem.65.9.3793-3799.1999 From NLM.

(38) Nair, R. V.; Bennett, G. N.; Papoutsakis, E. T. Molecular characterization of an aldehyde/alcohol dehydrogenase gene from Clostridium acetobutylicum ATCC 824. *J Bacteriol* **1994**, *176* (3), 871-885. DOI: 10.1128/jb.176.3.871-885.1994 From NLM.

(39) Raganati, F.; Procentese, A.; Olivieri, G.; Russo, M. E.; Salatino, P.; Marzocchella, A. MFA of Clostridium acetobutylicum pathway: the role of glucose and xylose on the acid formation/uptake. *Chemical Engineering Transactions* **2014**, *38*, 337-342.

(40) Lonkar, S.; Fu, Z.; Holtzapple, M. Optimum alcohol concentration for chain elongation in mixed-culture fermentation of cellulosic substrate. *Biotechnol Bioeng* **2016**, *113* (12), 2597-2604. DOI: 10.1002/bit.26024 From NLM.

(41) Tomlinson, N.; Barker, H. A. Carbon dioxide and acetate utilization by clostridium kluyveri. I. Influence of nutritional conditions on utilization patterns. *J Biol Chem* **1954**, *209* (2), 585-595. From NLM.

(42) Los, G. V.; Encell, L. P.; McDougall, M. G.; Hartzell, D. D.; Karassina, N.; Zimprich, C.; Wood, M. G.; Learish, R.; Ohana, R. F.; Urh, M.; et al. HaloTag: A Novel Protein Labeling Technology for Cell Imaging and Protein Analysis. *ACS Chemical Biology* **2008**, *3* (6), 373-382. DOI: 10.1021/cb800025k.

(43) Briegel, A.; Li, X.; Bilwes Alexandrine, M.; Hughes Kelly, T.; Jensen Grant, J.; Crane Brian, R. Bacterial chemoreceptor arrays are hexagonally packed trimers of receptor dimers networked by rings of kinase and coupling proteins. *Proceedings of the National Academy of Sciences* **2012**, *109* (10), 3766-3771. DOI: 10.1073/pnas.1115719109 (acccessed 2022/04/25).

(44) Fast Alan, G.; Papoutsakis Eleftherios, T.; Kelly Robert, M. Functional Expression of the Clostridium ljungdahlii Acetyl-Coenzyme A Synthase in Clostridium acetobutylicum as Demonstrated by a Novel In Vivo CO Exchange Activity En Route to Heterologous Installation of a Functional Wood-Ljungdahl Pathway. *Applied and Environmental Microbiology 84* (7), e02307-02317. DOI: 10.1128/AEM.02307-17 (acccessed 2022/04/25).

(45) Pyne, M. E.; Bruder, M.; Moo-Young, M.; Chung, D. A.; Chou, C. P. Technical guide for genetic advancement of underdeveloped and intractable Clostridium. *Biotechnol Adv* **2014**, *32* (3), 623-641. DOI: 10.1016/j.biotechadv.2014.04.003 From NLM.